Energy assessment of urban development scenarios for Merketal II

Master thesis submitted during the summer semester 2020 / 2021

At the Bauhaus University Weimar

Faculty of Architecture and Urban planning

M.Sc. Integrated Urban Development and Design

Author : Bardo Salgado Henríquez

Matriculation: 121911

Examiners

1st examiner	Vertr. – Prof. Dr. Sven Schneider
2nd examiner	Dr. – Ing. Martin Bielik

Place, Date	Weimar, August 2021

Content

Table of figures and tables

1 Introduction

1.1 Motivation and problem statement

Urban development and how cities are built have a significant impact on the energy demand and CO_2 emissions (Oliveria & Silva, 2013). Just in Germany, it is estimated that cities are responsible for about 80% of the country's end-energy demand. The energy generation sector alone contributes with 41% of total CO_2 emissions. More importantly, the shape of the spatial development and urban form has a great potential in reducing demands and increasing efficiency (Asarpota & Nadin, 2020).

Diverse studies on the urban form have stressed the importance of urban design when it comes to maximizing on-site renewable energy production and reducing CO_2 emissions. Though the results of simulations studies may vary, a review on the impact of urban form and energy performance suggests that the influence of building form on building energy use could be around 100 – 120%. (Quan & Li, 2021) . The link between urban form and energy performance has been established through passive and active constraints of physical geometries (Shi et al., 2017).

In existing urban areas, actions are focused on renovation measures and changes to the energy supply system. In contrast, new urban development projects pay attention to optimizing the building envelope and surfaces for the use of renewable energies such as photovoltaics, solar thermal, or environmental heat (Müller, 2020). A study on this topic found out that the generation of power through PV systems not only depends on the insolation intensity of the context and technological progress in PV systems but also on the availability of suitable spaces its deployment (Zhang et al., 2019). Since such passive characteristics are typically fixed at an early-stage phase, the need for energy performance assessment methods for decision-making has been stressed out (Nault et al., 2015).

In recent days, the city of Weimar has announced the development of a new urban quarter project in the area of Merketal. The project "Merketal II" intends to be the model project for the future housing of Weimar. The objectives of this neighborhood are the meaningful reduction of energy use, strengthening renewable energy sources, and increasing life quality (Stadt Weimar, 2021). The project is aligned with Weimar's climate protection objectives, targeting the reduction of energy consumption, an increase of energy efficiency, and the share of renewable energies in the city (Stadt Weimar, 2011).

Though it has been stated that the development will take place on 14 hectares located in the south of Weimar, by the time this work started, no urban design or whatsoever showing plans of the physical development of this area was available. Therefore, further research is needed to estimate the impact and assess the energy performance of this new project.

1.2 Literature review

This section presents a literature review of studies on urban form and energy performance, highlighting measures, approaches, and tools used in this field. This review is not an exhaustive revision but rather considerations from previous research that paves the way for assessing the energy performance of the urban form.

A systematic review of measures and methodologies on urban form and energy use found out that urban form and energy use have been approached differently based on how the concept of urban form is understood. (Quan & Li, 2021). Since the urban form[1] encompasses physical and no-physical characteristics (Dempsey et al., 2008), the relationship with energy can consider different elements ranging from building materials to the street and spatial arrangement types.

The work developed by (Silva et al., 2017) studies the relationship between urban form and energy at the city scale. The literature review collects relevant indicators and metrics that influence the energy demand in the building and transport sector. The energy demand is defined as the energy needed for heating and cooling, while the urban form attributes refer to the urban settings that are effectively built up. The conclusion of the qualitative review summarized broad prescriptions on how the urban environment should be organized to reduce the energy demand. Such prescriptions are concerned with the principles of passive design involving the arrangement of the physical form to increase benefits of ambient energy (heating, lighting, and ventilation) and reduce the demand for conventional fuels (Altan et al., 2016; Littlefair, 1998).

In addition to the energy demand benefits, a study of the impact of urban block typologies on energy use (Zhang et al., 2019) analyzed the potential of energy generation through photovoltaic systems (PV). The capacity to generate energy through PV systems is determined by the insolation intensity of the context and technological progress in PV systems and the availability of suitable spaces for its deployment. For this, the urban form was analyzed at the urban block scale. Thirty generic building forms belonging to six representative urban block typologies were examined regarding solar radiation (PV potential) and building energy use (EUI). The urban blocks' geometric and planning parameters were estimated to find correlations and establish relations with the performance indicators. The findings report that solar energy harvesting potential varies

[1] Elements of the urban form are the following: density, transport infrastructure, housing/building type, land use and layout. The non-physical characteristics include size, shape, scale and distribution.

significantly across the six generic urban block typologies. The courtyard typology (medium-rise linear buildings) and the hybrid typology consistently have more significant solar potential than the alternatives. In terms of geometric parameters, the Sky View Factor (SVF) and Sky Exposure Factor (SkyEF) could potentially be adopted as proxy factors for the preliminary evaluation of solar harvesting potential. At the same time, the roof-to-area ratio, site coverage, open space ratio, and roof-to-envelope area ratio become effective predictors for solar energy harvesting potential. Compacity was found to be a significant predictor of EUI without PV deployment. These correlations should be considered cautiously since the simulation study used Singapore's weather data, and planning and geometric parameters were not directly examined concerning the performance parameter.

The pertinence to use geometric parameters to establish energy performance assessments was studied by (Nault et al., 2015). Here the urban form and energy performance at the neighborhood scale was analyzed. The work builds on the argument that solar exposure strongly influences building energy performance. To prove that, different building performance criteria and evaluation metrics were identified and later compared. The performance criterion of buildings considers passive and active solar categories, while the evaluation metrics were categorized as geometry-based, external solar-geometry-based, and entire climate–geometry-based[2]. The findings show that surface-to-volume (SVR) and window-to-floor ratio (WFR) perform best as indicators for the heating need and spatial daylight autonomy, respectively. The overall best indicator for all performance criteria appears to be the annual radiation per floor area; however, using easily computable metrics as performance indicators can have significant drawbacks. For instance, using the SVR or radiation per envelope area for the optimization (maximize) of a design scenario can increase 6% and 20% heating need, respectively. Therefore, the optimization of the urban form should carefully consider the use of geometric measures. A later work by (Natanian, 2018) draws some conclusions on the correlation between the shape factor and energy balance potential. Several trade-offs in the context of coastal Mediterranean climates are highlighted. Higher shape factors correlate with the impact on average load match (Av. LM), but considering this as a standalone indicator is depictive. Cases of similar SVR ratios but with a higher ratio between roof and façade surfaces result in substantially higher energy production yields and potentially higher energy load balances. Another trade-off is reported between visual comfort and energy to load

[2] 1) Selected geometry-based metrics: density, compactness, passive zones and glazing ratio; 2) Selected external-solar geometry-based metrics: percentage of exposed surface area receiving irradiation or illuminance level (different threshold values for photovoltaic and thermal considering roof/ wall surfaces); 3) Selected full-climate geometry-based metrics: annual heating/cooling need per floor area (kWh/ m^2), and annual energy production on roof/ façade per floor area (kWh/ m^2)

balance. While a higher window-to-wall ratio (WWR) improves daylight levels and reduces artificial lighting loads, it simultaneously increases the cooling loads and reduces energy production potential in vertical façades. Following the previous study, a multi-objective optimization (MOO) was carried out to minimize the energy demand and maximize the energy supply. The last was done through the maximization of geometric exposure index-geometric shading index (GEI-GSI[3]) and solar radiation exposure index- solar shading index (SEI-SSI), respectively (Natanian & Wortmann, 2021). The main result reported that the façade-to-surface ratio showed the highest correlation with PV potential supply and the effective use of area-weighted exposure and shading indices as prediction metrics of energy demand, supply, and energy balance.

The optimization studies mentioned above fall inside the energy-driven urban design. Through passive and active energy-driven constraints, the energy-driven urban design looks to decrease energy demand while maintaining a high human comfort level (Shi et al., 2017). Passive energy design constraints organize the urban form to reduce heating demand or gain more solar heat, while active urban design constraints shape the urban form to meet a specific requirement of active energy infrastructure. The latter can be exemplified by optimizing land use distribution and land use ratio to reduce the operational and infrastructure costs of a district cooling system in high-density cities (Hsieh et al., 2017).

The impact of passive and active approaches concluded that passive design strategies should be prioritized since they are more efficient in terms of energy-saving than active strategies (Kang et al., 2015). The energy-saving potential of active strategies like automatic lighting, dynamic exterior blinds, and controlled ventilation with heat recovery is influenced by physical characteristics as orientation and WWR. Therefore, passive strategies (as orientation, fenestration, room relocation) should be addressed and assessed in the early stages of a design that informs the decision-making (Nault et al., 2015) since they require significant effort and time to redesign or change.

In terms of methodology, the impact of the built environment on energy use has been approached under the scope of the life cycle assessment (LCA). The LCA is an internationally standardized methodology that can assess the environmental impacts of products during their lifetime (Soukka et al., 2020). At the urban scale, the LCA quantifies the resulting energy use and greenhouse in the following categories: embodied, operational, transportation, and consumption (Anderson et al., 2015). Some energy use analyses overlap between the building and urban scale; therefore, an induced impact category was introduced to bridge both of them. This category considers the

[3] Geometric shading index GEI was evaluated for rooftops and geometric shading index GSI for east and west façade.

location of the building and mobility patterns for the assessment of the environment. Despite the previous, the operational stage of the built environment becomes relevant since around 84% of the energy is used during this stage. (Adalberth, 1997).

1.1 Research objectives and work structure

Recognizing the impact of urban form on energy performance and the lack of a project for Merketal II, this work presents five possible urban development scenarios for Merketal and the assessment of their energy performance. To that end, five layouts representing different urban development scenarios for the site area in Merketal are based on existing urban block typologies, representing possible local development scenarios. The analysis was carried out using computational radiation and energy simulations in the operational stage of the development for one year. The energy performance features considered photovoltaic energy potential (PVE) and energy use (EU), while geometric and planning parameters are also estimated for each scenario. This case of study aims to answer the following question:

- What is the impact in terms of energy use and solar harvesting potential of different urban development scenarios in Merketal?

The first part introduces the work, followed by a literature review on the relationship between the built urban form and energy performance. The second section explains the methodology, describing the independent variables and performance indicators used in this work and specifications on simulations and models. Section three presents the results and findings of the analyzed scenarios and the optimization of one alternative. In the final part, the results of energy use and solar harvesting potential are discussed as well as the limitations of this work.

2 Methodology

2.1 Analytical approach

In order to assess the energy performance of different urban development scenarios, this work used the methodology in Figure 1. The first part presents the collected information about climate and geometric data of the city of Weimar, and it describes the possible urban development scenarios for Merketal. The second part describes the geometric and planning parameters considered as well as the performance indicators, giving some specifications about the solar radiation and building energy use models.

Figure 1 Methodology

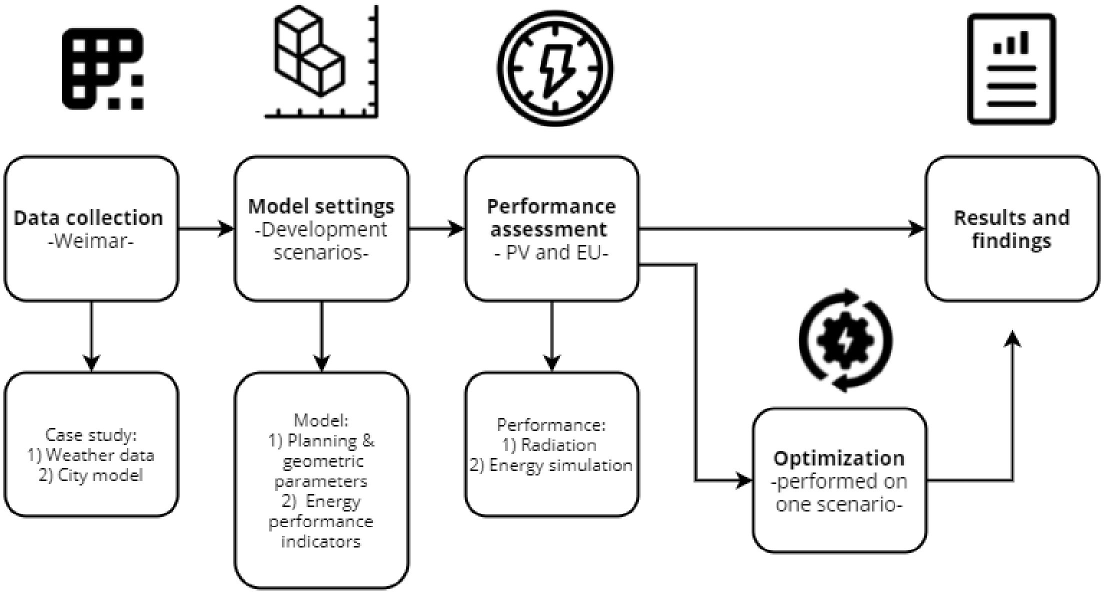

2.1 Data Collection

2.1.1 Case study: Merketal

"Merketal II" intends to be the model project for the future housing of Weimar. The meaningful reduction of energy use, strengthen of renewable energy sources (particularly solar energy) and increase of life quality are the objectives of this new neighborhood in the south of the city. Here the implementation of energy supply, passive housing, and sustainable mobility are essential aspects to be integrated (Stadt Weimar, 2021).

The project is aligned with Weimar's climate protection objectives, targeting the reduction of energy consumption, an increase of energy efficiency, and major share of renewable energies in the city (Stadt Weimar, 2011). It is estimated that the city has an energy-saving potential of around

30% for heating and 10% for electricity. Additionally, it is projected that 60% of Weimar's energy demand can be covered by renewable sources, specifically PV systems. The potential for geothermic sources is high due to the soil conditions; however, there is a mismatch between supply and demand locations.

Although no physical project is known by the time this work started, some of the first released specifications consider 20% of the total housing units as social housing, a KfW-Effizienzhaus 40 [4] energy efficient standard for buildings, as little as possible pavement and sealed surfaces, and the deployment of PV systems on all roof surfaces (Stadt Weimar, 2020).

The Merketal project considers the development of a new neighborhood on 14 hectares in the south of Weimar. The project area is located near the city's hospital, supermarket, and Ilm Park. The surface is currently used for agricultural purposes and is characterized by an irregular terrain where 60% of the land has a slope above 6% (Figure 2). Despite being marked as a housing zone in Weimar's land-use plan, the neighbors have shown resistance to this project.

Figure 2 Merketal location (left) and terrain slope analysis (right)

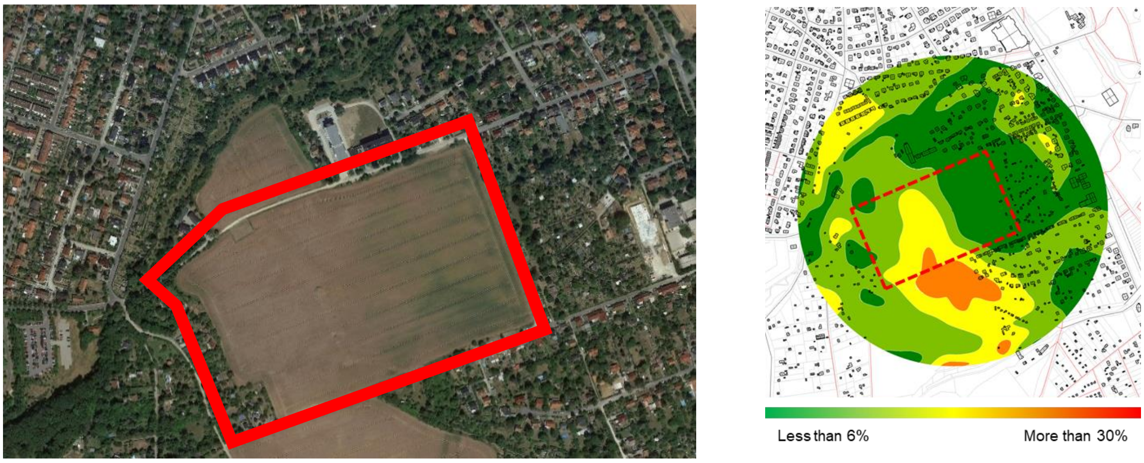

Source: Google Satellite and InfAr

2.1.2 Climate conditions

The climate data for the city of Weimar comes from an integrated surface database (NCEI ISD) in EPW (energy power weather) file format. This database comprises 8,760 hours of weather records between 1940-2006, representing some limitations since the information does not consider data of recent periods. This information is essential for further simulations of solar radiation and building energy use.

[4] Energy standard for buildings that reduce 60 % the consumption of primary energy and the supply of energy comes from renewable sources.

The total solar radiation is particularly important for the PV design. Solar radiation is the power from the sun that reaches a surface and is classified as direct and diffuse radiation (Stein et al., 2012). Periods with low solar radiation (i.e., rainy seasons, cloudy sky, or short periods of sunlight) affect the efficiency of PV systems (Ghazi & Ip, 2014). The mean daily radiation shows a single peak in June when about 6 kWh/ m^2 are received Figure 3. The Skydome patches show that the southeast part is the most intense source of solar radiation (Figure 5).

The temperature impacts the thermal comfort of a person and therefore has significant implications in building energy use. Seasons with extreme temperatures will present higher energy consumption (heating or electric) (Zarco-Soto et al., 2020). According to the ASHRAE[5] and Köppen-Geiger classification (Kottek et al., 2006), Weimar is classified as a cool-humid climate zone (5A) with a warmer temperate climate (Cfb). Considering thermal comfort values (Bröde et al., 2011) and the temperature records of Weimar, the energy used for heating might increase from October-February, where mean temperatures are under cold stress < 9° C (Figure 4).

The wind is another factor that directly affects a person's thermal sensation and, therefore, the energy demand (Dec et al., 2018). A general overview of the wind speed data reveals that the highest wind speeds, around 9m/s, are coming from the west/south direction (Figure 5).

2.1.3 City model

The chair of Computer Science provided the urban model in Architecture (InfAr) whic includes buildings, plots, elevation model, and street network of Weimar. The primary source of the model was the geoportal of Thüringen. The model's level of detail corresponds to LOD1 standard, meaning that buildings were represented as volumes with flat roofs. Additional specifications are given in Figure 6.

[5] American Society of Heating, Refrigerating and Air-Conditioning Engineers

Figure 3 Mean of daily radiation per month

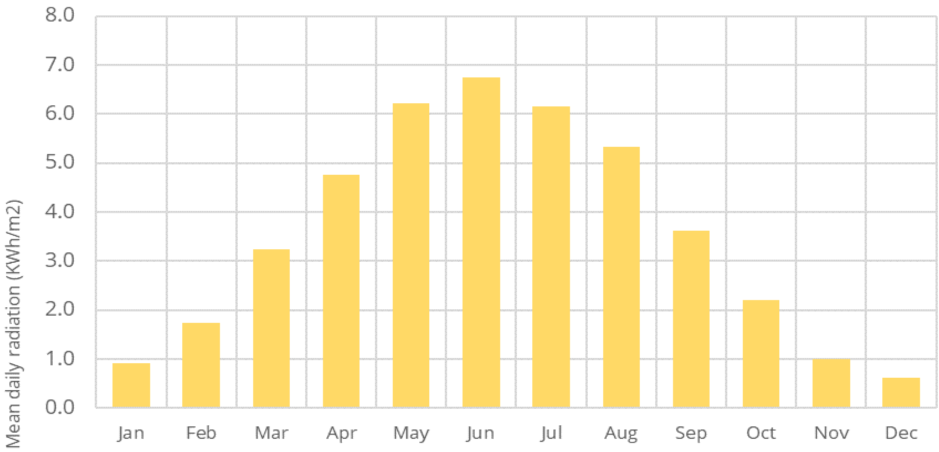

Source: (Climate.OneBuilding.Org, 2021)

Figure 4 Highest, mean, and lowest daily temperature over a year

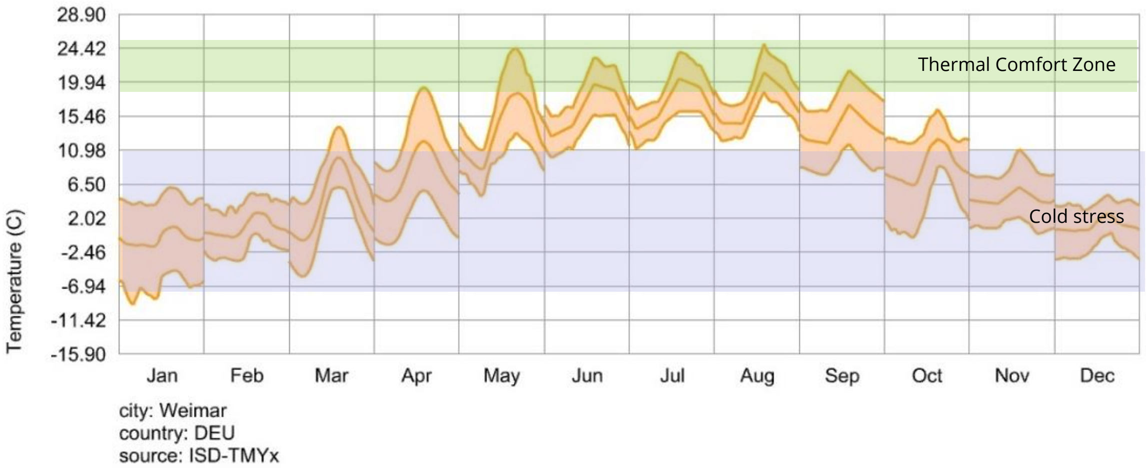

Source: (Climate.OneBuilding.Org, 2021)

Figure 5 Skydome radiation values (left) Wind speed (right)

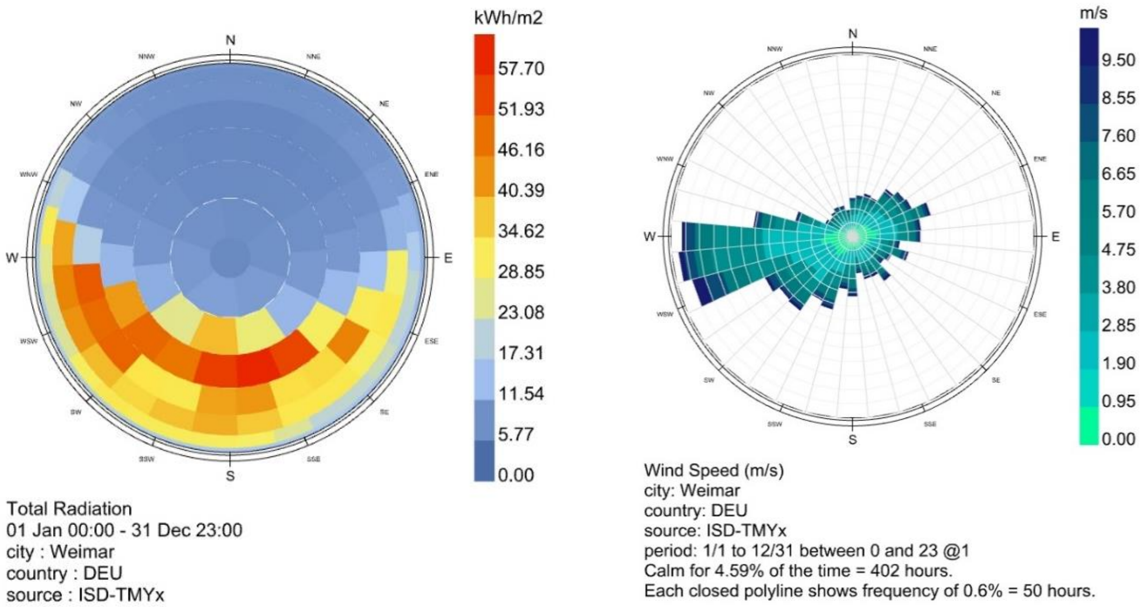

Source: (Climate.OneBuilding.Org, 2021)

Figure 6 Weimar city model specifications

Buildings

- modeled in LOD1 (Extruded footprints)
- buildings are differentiated by function in separate layers
- buildings are positioned based on their elevation

Plots

- plots are differentiated by function in separate layers

Street network

- streets are differentiated by type (pedestrian, car) in separate layers
- simplified street network without parallel lines, changing roundabouts to crossings, merging all nodes in the distance < 10m.

Topography

- Based on DGM (1m raster), resampled to DGM50
- Airborne Laser scanning with buildings filtered out

2.1.4 Development scenarios

This section proposes different urban development scenarios that could be implemented in Merketal. Each development scenario takes into account a different urban block typology pattern. The block typologies represent distinct residential development that could be considered for the project area. Thus, the urban block becomes the unit of analysis, and it is regarded as the basic component of the urban fabric that can be described in terms of geometric and planning parameters (Zhang et al., 2019).

Considering the housing type matrix (Loga et al., 2015), the following urban block typologies were identified: 1) detached house, 2) townhouse, 3) apartment building, 4) large apartment building, and 5) skyscraper. Subsequently, five urban block types from the current built environment of Weimar were selected as the model urban blocks.

Several studies from the literature review conducted their analysis implementing a "normalization and replication" approach. This approach examines the theoretical performance of a given built form in an ideal homogeneous context allowing to give generalizable findings when comparing the performance of alternative urban block typologies (Zhang et al., 2012). However, this case-specific study considers urban blocks from the city of Weimar as models for the development scenarios on the project site. The reasons to implement this approach were 1) it helps to exclude designs that are unlikely to be introduced in the urban setting of a city like Weimar; and 2) it reflects the local existing built environment, cultural preference, local climate, and local governmental regulatory codes (Shi et al., 2021). Figure 7 shows the urban block typologies considered for the scenarios. The skyscraper type was not included as a model urban block since such a pattern does not belong to the vernacular practice of urban design in Weimar.

Figure 7 Urban block types

UBT01

apartment building

UBT02

apartment building

UBT03

townhouse

UBT04

detached house

UBT05

large apartment building

The above block typologies served as models to propose urban development scenarios in Merketal. Later a grid layout considering a standard size for blocks and streets was projected on the study area. The size of the urban block was set to 100m X 100m with street sections of 15m. The proposed array resulted in a layout of 11 urban blocks. The block division prioritized Merketal street since this is the most consolidated street segment in the surroundings. The geometry was adjusted in the area facing Albert Kunz street (Figure 8). Once the urban block typologies and urban layout were set up, the five urban development scenarios were then modeled in Rhino using Grasshopper (Figure 9).

Figure 8 Urban layout projected on Merketal site

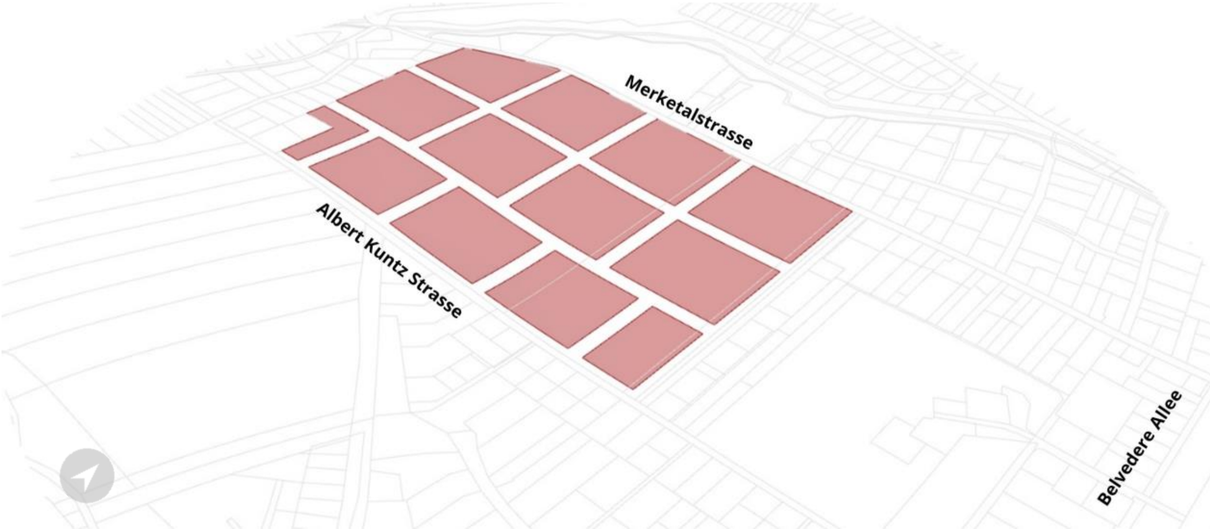

Figure 9 Urban scenarios projected on Merketal site

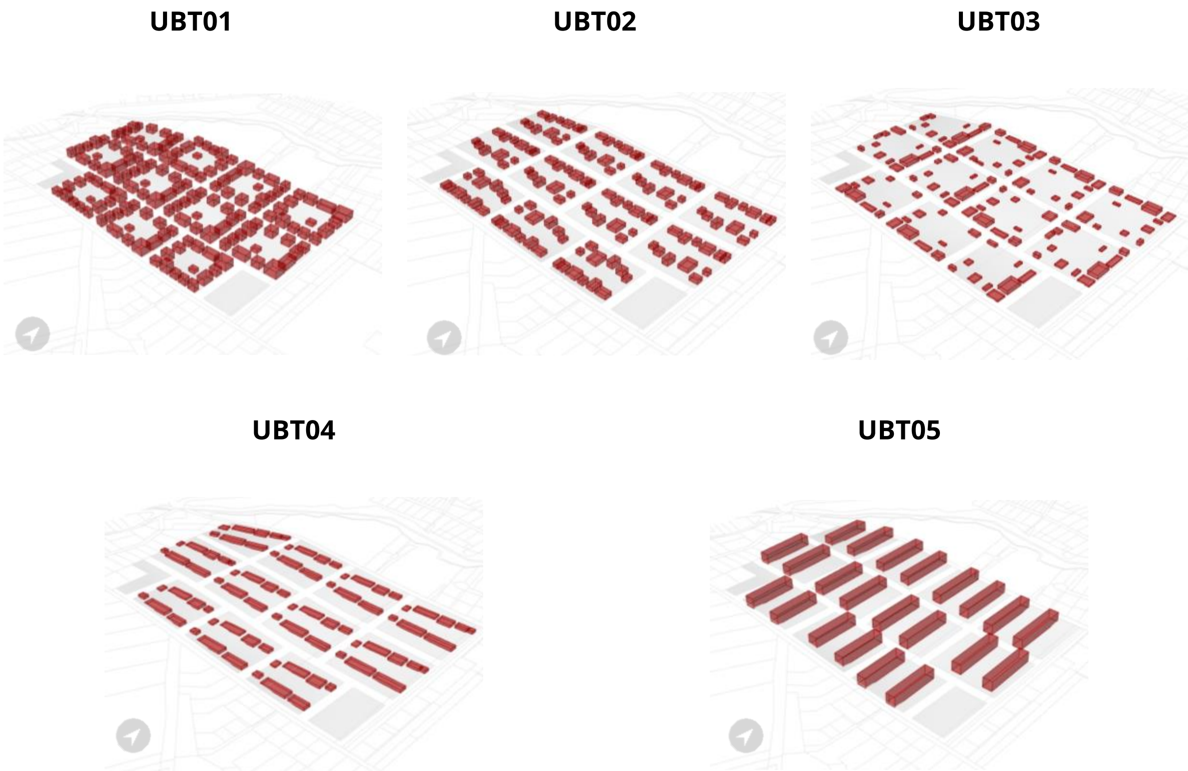

2.2 Model parameters and indicators

A set of geometric and planning parameters that describe and measure the urban blocks was calculated for each urban scenario. The following section will explain the calculation of each parameter and the relevancy for the energy assessment.

2.2.1 Urban parameters

The ground space index (GSI), floor-area ratio (FAR), and open space ratio OSR measure the density of the urban form (Berghauser Pont & Haupt, 2009). The GSI corresponds to the built coverage of a site area, the FAR represents the building intensity, and the OSR is the number of outdoor areas or non-built spaces in a given site. These metrics were calculated at the urban block scale in each urban development scenario.

The influence of these parameters on energy use is differentiated and complex. The GSI alone shows a direct relationship to energy use, meaning the more GSI, the more EU. This previous might represent a trade-off with PV since a more extensive building coverage represents more harvested solar energy potential for the latter. The impact of FAR on energy use is stated as a complex relationship suggesting the existence of thresholds under certain conditions (Quan & Li, 2021). In addition to the previous, the number of storeys (SN) and Gross floor area (GFA) were considered for a more detailed description of the urban form.

Figure 10 Urban parameters

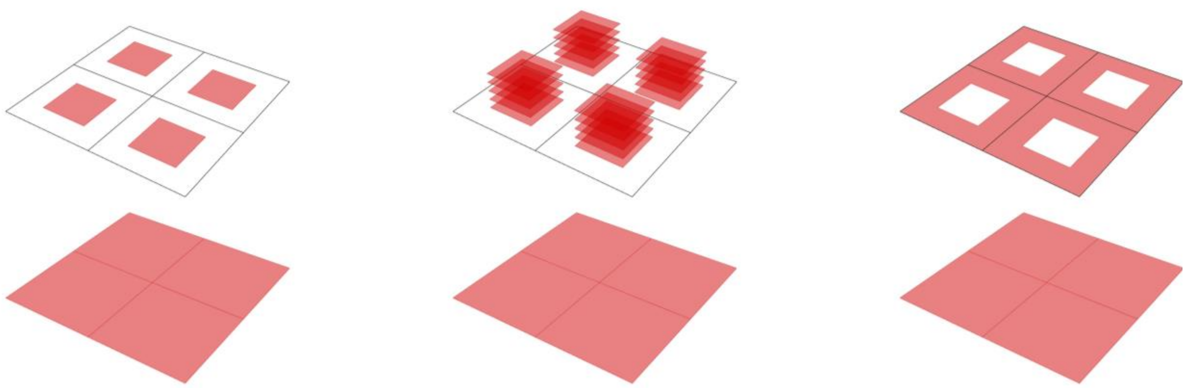

$$GSI = \frac{Block\ building\ footprint\ area}{Block\ area} \qquad FAR = \frac{Block\ gross\ floor\ area}{Block\ area} \qquad OSR = \frac{Open\ surface\ area}{Block\ area}$$

2.2.2 Geometric parameters

The sky exposure factor (SkyEF), surface-to-volume ratio (SVR), and orientation (OR) were considered as geometric parameters. Those were first calculated for the building volumes and later were aggregated at the urban block scale.

The SkyEF represents the degree of exposure of a specific surface and is relevant to analyze the radiation exchange between urban surface and sky (Zhang et al., 2012). In this case, it was calculated only for the facades since it is assumed that roof exposure has a complete exposure (1) and not over shading is occurring. For facades, both extreme low (0) and high (1) sky exposure (SE) represent not desirable conditions; therefore, only those surfaces with a SE between 0.2 and 0.4 were normalized and considered appropriate.

The SVR is a measure of compactness defined as the building envelope area to the building volumes where values near 0 are considered compact (Araji, 2019). Here is noteworthy that SVR does not always indicate energy-efficient conditions for the buildings, and there are more accurate form shape indicators for this[6] (Lylykangas, 2009). Since this work is additionally considering an energy simulation, this parameter only indicates geometrical compacity. Regarding the orientation, the absolute rotation angle between the longest building axis and the horizontal x-axis was taken into account as orientation angle. This calculation was carried out for each building, and later an average value was estimated for each urban block.

The orientation at the building scale determines the amount of solar radiation on each of its facades and, consequently, the requirements for space heating and cooling (Silva et al., 2017). According to (Hemsath, 2016) the orientation is the most critical design parameter because it determines the building energy requirements. The OR was estimated as the angular difference between the x-axis and largest building axis.

[6] Heat Loss Form factor have better correlation to indicate the building energy demand.

Figure 11 Geometric parameters

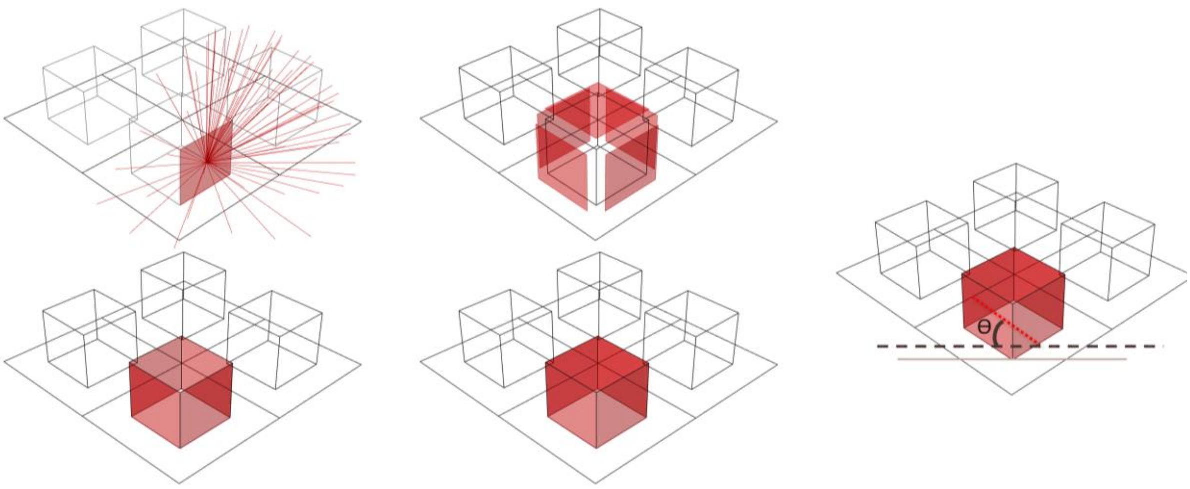

$$SkyEF = \frac{0.2 < SE < 0.4\ Facade\ area}{Building\ facade\ area}$$

$$SVR = \frac{Building\ envelope\ area}{Building\ volume}$$

Figure 12 Urban and Geometric parameters per urban block typology

ID	Urban Block type	Parameter
UBT 01	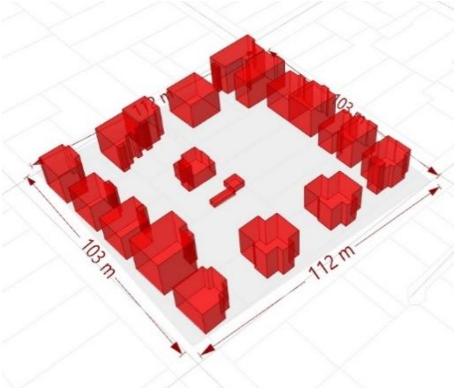	GSI =0.23 FAR =0.49 OSR =0.77 SkyEF =0.44 SVR =1.61 OR =70.18
UBT 02	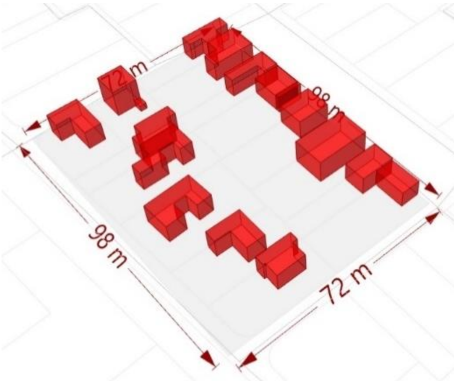	GSI =0.32 FAR =1.36 OSR =0.68 SkyEF =0.42 SVR =1.30 OR =65.75
UBT 03	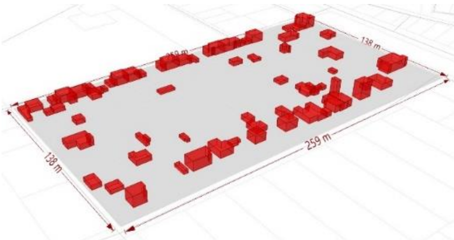	GSI =0.13 FAR =0.2 OSR =0.87 SkyEF =0.33 SVR =2.38 OR =22.65
UBT 04	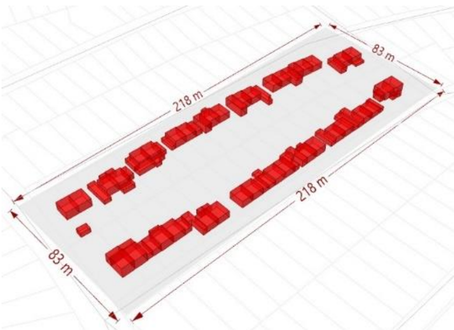	GSI =0.22 FAR =0.29 OSR =0.78 SkyEF =0.20 SVR =2.47 OR =40.17
UBT 05	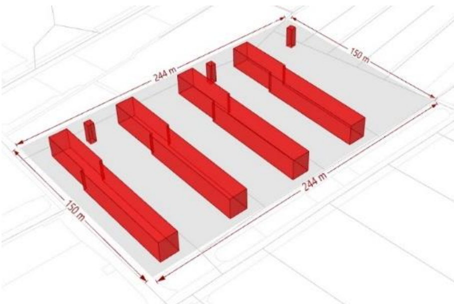	GSI =0.21 FAR =1.03 OSR =0.79 SkyEF =0.43 SVR =0.84 OR =2.86

2.3 Energy performance indicators

The performance indicators were calculated following the steps of previous studies (Natanian & Wortmann, 2021; Zhang et al., 2019). The building energy use and solar harvesting potential indicators were calculated with computational simulations using Climate Studio.

ClimateStudio is a licensed software for daylighting, electric lighting, and thermal simulations. It supports different environmental analyses for buildings and neighborhoods, including annual illuminance simulations for LEED certifications and radiation map analysis for design studies (Solemma LLC, 2021). ClimateStudio is built on Radiance and Energy plus engines for radiation and energy simulations, and it was chosen due to its integration with Rhinoceros-Grasshopper and quicker simulation time.

Depending on the type of analysis, the simulation in Climate studio required a different level of detail of the geometric models. For the energy simulation, the geometric models considered the storeys of the buildings, and each storey represented a thermal zone. The solar radiation analysis required only a sensor grid of 3.6m on the building envelope.

In addition, to reduce computational time, the original geometries were simplified and normalized as other studies have suggested (Zhang et al., 2012). This approach was applied to buildings and urban blocks and involved transforming irregular shapes into rectangles keeping the original orientation and height (Figure 13). This transformation reduces the number of surfaces and geometries to be analyzed in the simulation studies.

2.3.1 Building energy use

The building energy use (EU) and energy use intensity (EUI) were considered metrics for the building energy performance. The energy use corresponded to the utilized energy during the operational stage over one year. Operational energy is the energy required during the entire service life of a building and accounts for the most significant energy use in the life cycle of a typical building. Operational energy considers heating, cooling, lighting, ventilating systems, and household appliances. During such phase, buildings gain energy through solar, persons, warm water, process, and heating system; And they lose energy due to transmission, ventilation, leakage, and sewage (Tuladhar & Yin, 2019).

Figure 13 Simplified geometries for energy models

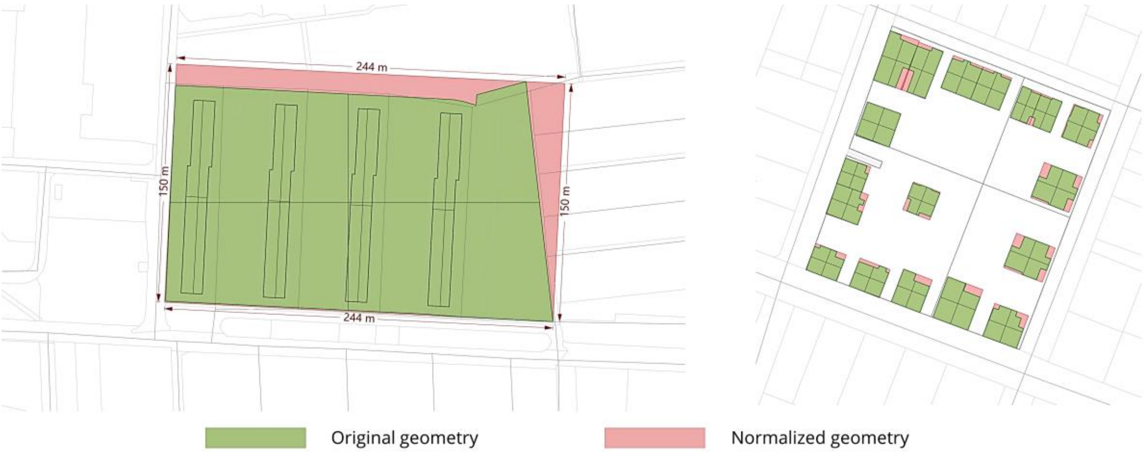

The second performance indicator (EUI) is calculated by dividing the EU by the total gross floor area. This indicator is used as a baseline to compare different buildings or previous performances (Yang & Choi, 2015).

The energy model requires geometric data, simulation inputs, and climatic data of the local context. Each block's energy simulations were conducted through an iterative process in Grasshopper using ClimateStudio and Anemone plugins. The buildings on each block were divided into storeys, and each storey was considered a thermal zone (Figure 14). A set of simulation properties regarding loads, HVAC[7], ventilation, water, and materials were assigned to each thermal zone. These properties were kept constants for all five scenarios and a fenestration ratio of 30% in all buildings' facades.

Figure 14 Building energy model (left) and simulation specifications (right)

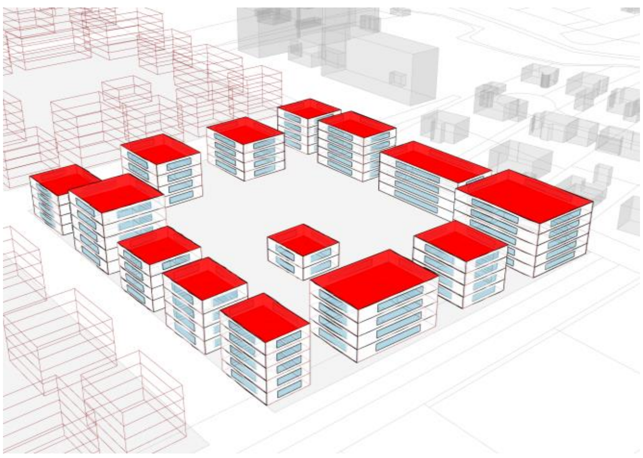

Settings		
Program		Multifamily housing
Window-to-wall ratio		0.3
HeatingSetpoint		20
CoolingSetpoint		26
Internal loads		
Equipment		7 W/ m2
Lighting		16 W/ m2
Occupancy		0.07 person/m2
Building construction		
Floor surface		0.25 mm concrete Wall with mineral wool
	U-Value	3.58 W/m2K
Wall surface		0.25 m concrete Wall
	U-Value	3.58 W/m2K
Window surface		Solarban 60 (2) on Starphire
	U-Value	3.22 W/m2K
	Transm.	0.5

[7] Heating, ventilation and air conditioned

2.3.2 Solar harvesting potential

The suitable surfaces for solar harvesting (SSSH) and electricity generated by PV systems (PVE) were considered performance indicators of solar harvesting potential. A radiation simulation was carried out to analyze the solar radiation on the building envelope of each scenario. The radiation analysis required a climate weather file, a sensor analysis grid, and a daylight model of scene layers for lighting simulation. The scene layers took into account the context building volumes and building footprints, while the sensor grid considered a 3.6m sensor grid on the building envelope surface. All those surfaces with solar radiation above 800 kWh/m^2 were considered SSSH (Shi et al., 2021) (Figure 15).

The PVE estimation was carried out only considering the rooftop surfaces above the solar radiation threshold. This simulation required the contextual buildings of the project site and the PV system settings. The energy generated was estimated for one year, and the efficiency of the deployed PV panels was set to 20%.

Figure 15 Visualization of the solar radiation analysis for one urban development scenario

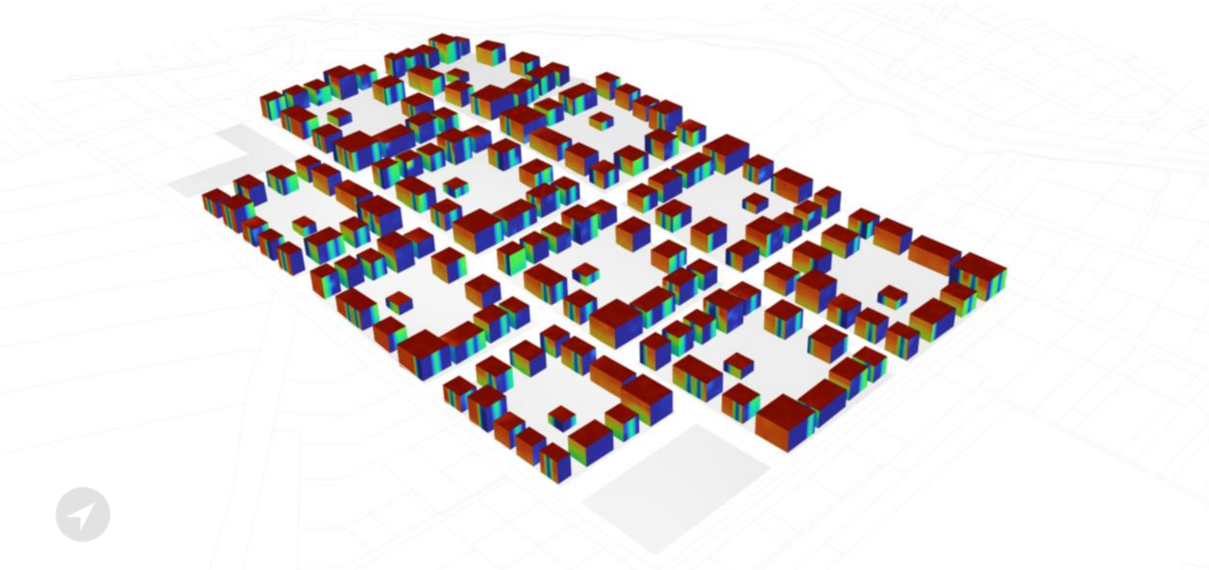

3 Results

Figure 16 and Table 1 show the geometric and urban parameters for each urban development scenario. In terms of intensity, both UBT01 and UBT05 have the highest FAR coefficients and gross floor area. There is a variation of around 5.3 times the gross floor area between the UBT01 and UBT04. The five scenarios show a similar proportion of open space regarding outdoor spaces, but the UBT01 scenario offers the lowest ratio. Regarding SkyEF, Table 1 indicates that compact typologies like UBT01and UBT05 recorded a more significant surface with desirable conditions than the spread alternatives.

Figure 16 Urban parameters for each scenario

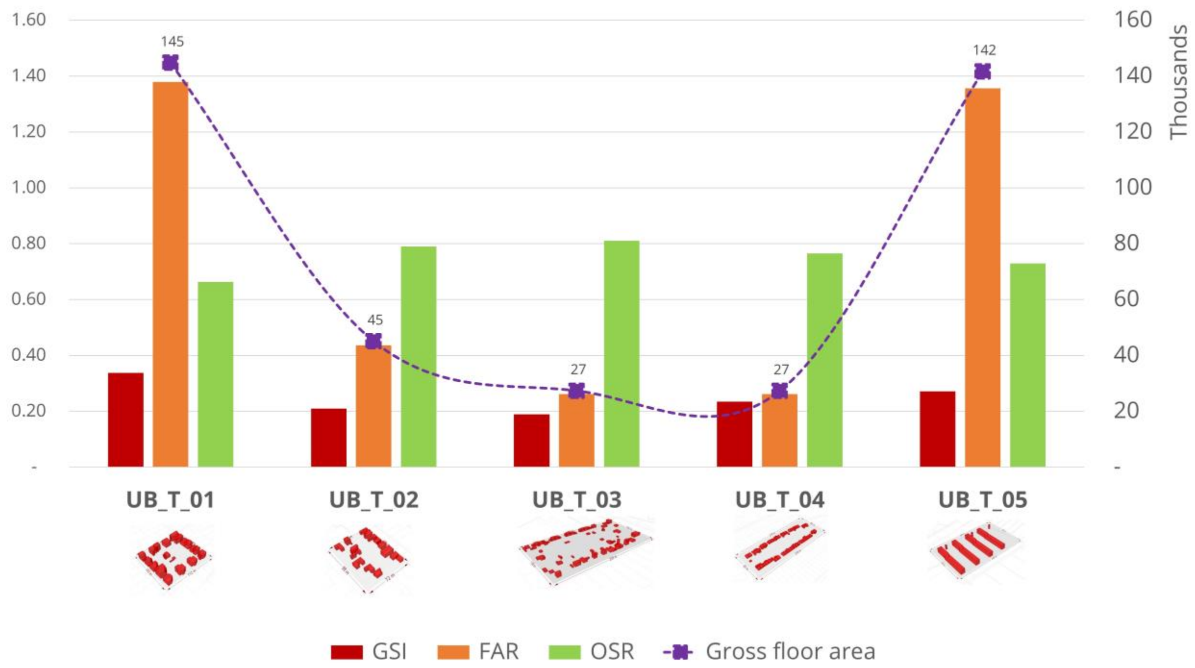

Table 1 Geometric and urban parameters of each urban scenario

		Ground Space Index	Floor Area Ratio	Open Space Ratio	Gross Floor Area (m)	Surface to Volume ratio	Sky Exposure Factor	Average Orientation (°)
	UB_T_01	0.34	1.38	0.66	144,751	0.45	0.37	38.07
	UB_T_02	0.21	0.44	0.79	45,066	0.63	0.32	52.68
	UB_T_03	0.19	0.26	0.81	27,326	0.97	0.22	40.95
	UB_T_04	0.23	0.26	0.77	27,258	0.82	0.14	31.44
	UB_T_05	0.27	1.36	0.73	141,679	0.28	0.30	67.09

3.1 Solar harvesting potential

Figure 17 shows the total PVE and normalized PVE for each urban design scenario. For the total PVE, the scenarios based on UBT 01 and UBT05 have the highest energy generation with around 1,282 MWh and 1,083 MWh, respectively, while UBT02 and UBT03 have the lowest PVE with 764 MWh and 697 MWh. The normalized PVE follows a similar trend, with UBT05 performing high and both UBT02 and UBT03 at the bottom; however, the UBT04 (37 kWh/m^2) slightly outperformed UBT01 (36 kWh/m^2). Additionally, analyzing the distribution of PVE by GFA of each scenario in Figure 18, it is observed that the UBT04 (33 kWh/m^2) outperformed all the alternatives. The previous suggests that under a development scenario based on UBT04, the share of PV energy sources is four times higher than the UBT05 (8 kWh/m^2).

Figure 17 Total and normalized PVE by development scenario

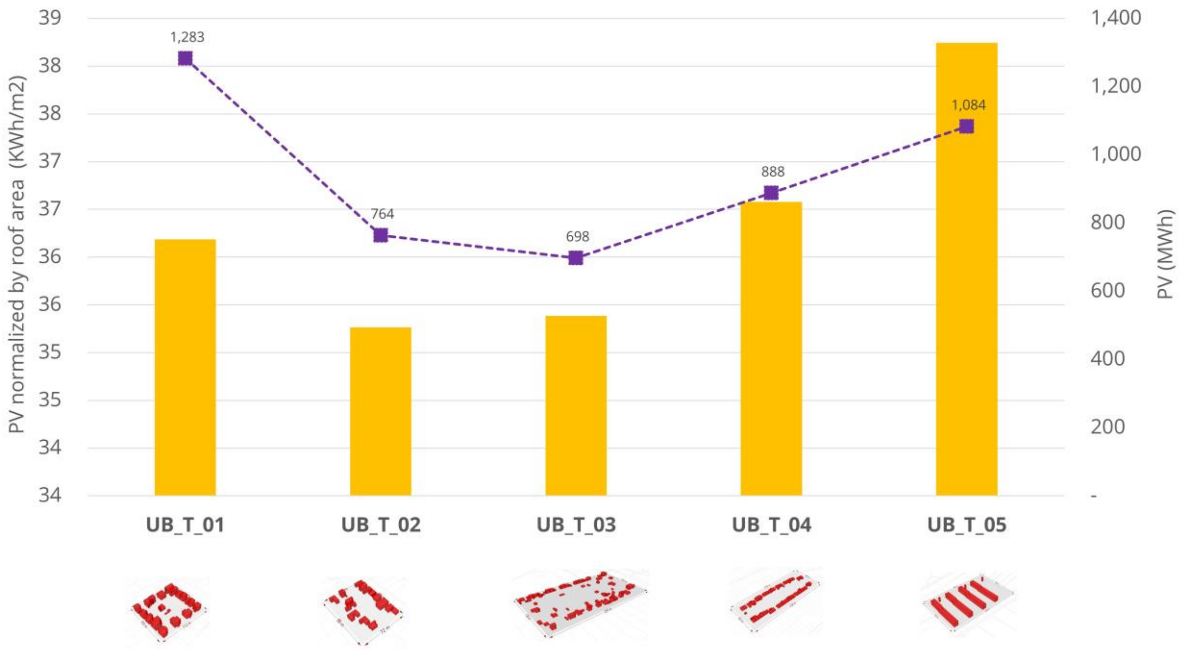

Considering the suitable surface for solar harvesting (SSSH), the urban form of UBT01 outperformed the other four since a higher amount of its building envelope received solar radiation above 800 kWh/ m^2. The other typologies have a similar amount of SSSH (Figure 19); however, it can be seen that UBT01 effectively uses only 71% of its SSSH, while the UBT05 and UBT04 alternatives use 87% and 84%, respectively. The previous indicates that the potential of UBT01 is not fully exploited.

Figure 20 shows the correlation of the total PVE with the urban and geometric parameters. In general, the OSR and SVR show a negative correlation with PVE. The GSI shows the strongest direct correlation with the PVE. In contrast, a negative correlation was found between the OSR and SVR, confirming that a higher OSR in compact urban forms offers less footprint area available for PV deployment. The SVR comparison indicates that compact urban forms as UBT01 and UBT05 produce the highest PVE. Here is noteworthy that the building orientation and SkyEF did not reveal a strong influence on energy generation.

Figure 18 PV energy distribution by gross floor area

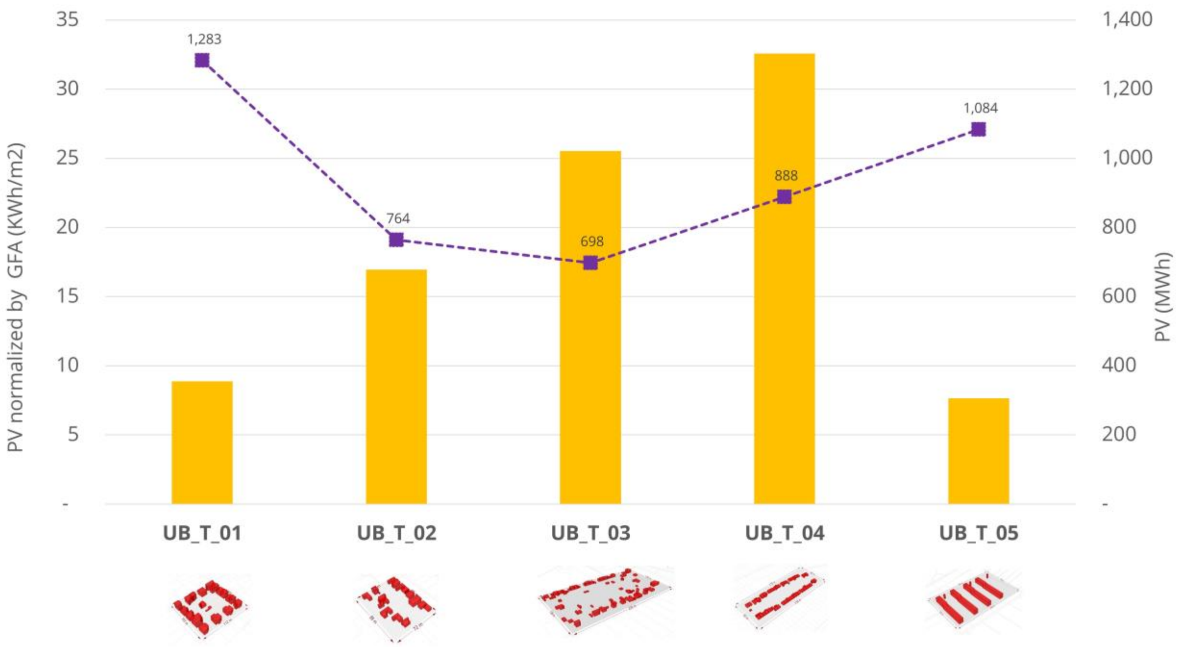

Figure 19 Surface suitable for PV and roof proportion

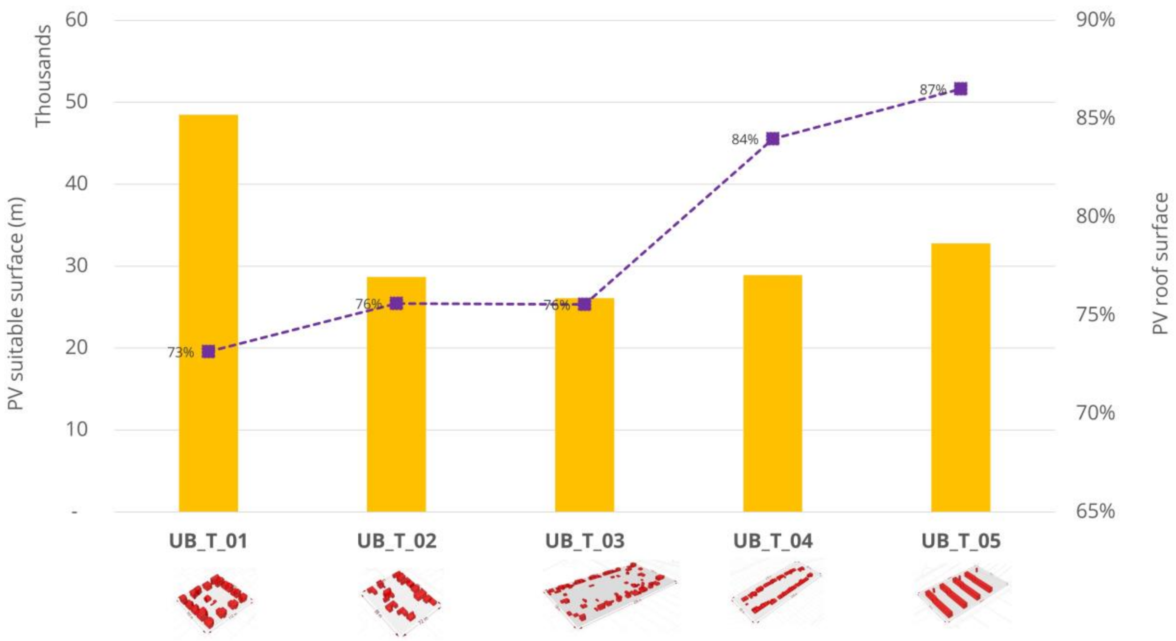

Figure 20 Relations between PVE energy generation and urban parameters

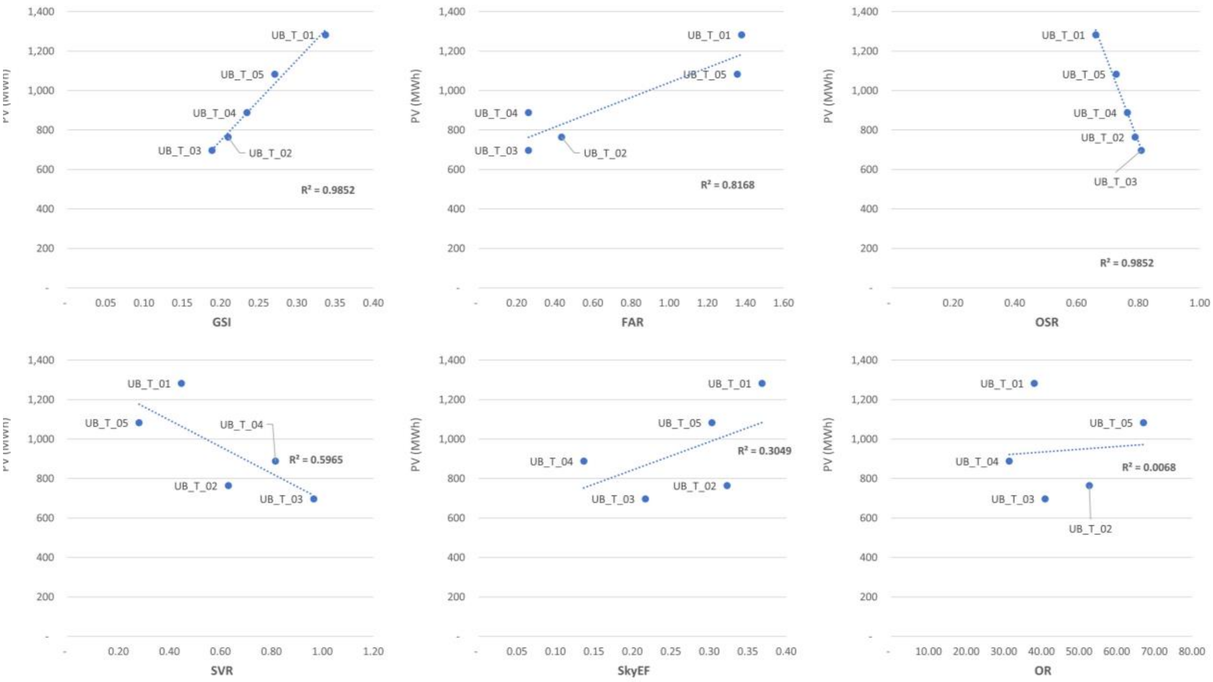

3.2 Energy use

The total building energy use and energy use intensity for the five urban development scenarios are shown in Figure 21. The UBT01 (28,398 MWh) and UBT05 (23,282 MWh) registered the highest total building energy use while UBT03 registered the lowest (5,736 MWh). There is a difference of five times the total energy use between the highest and lowest performance. Examining the result of EU normalized by GFA, it can be seen a difference of around 36% of the energy use intensity between the highest (UBT04) and the lowest (UBT05). In general, both UBT01 and UBT05 scenarios consumed less energy per m^2 than UBT04 (223 kWh/ m^2) and UBT03 (210 kWh/ m^2). Moreover, the UBT02 alternative showed a EUI of 196 kWh/ m^2, similar to UBT01 but with roughly 1,5 fewer times the total energy use.

Figure 22 takes a closer look at the categories of energy use intensity during a year. It can be identified that heating requires the highest energy following a seasonal pattern that reaches its peak in January.

The relationship between energy use and urban parameters is presented in Figure 23. In general, it is observed a positive correlation from most urban parameters excepting the OSR and SVR, which registered a high negative correlation with the EU. On the opposite, the GSI and FAR show a high direct correlation.

Figure 21 Energy use and energy use intensity by development scenario

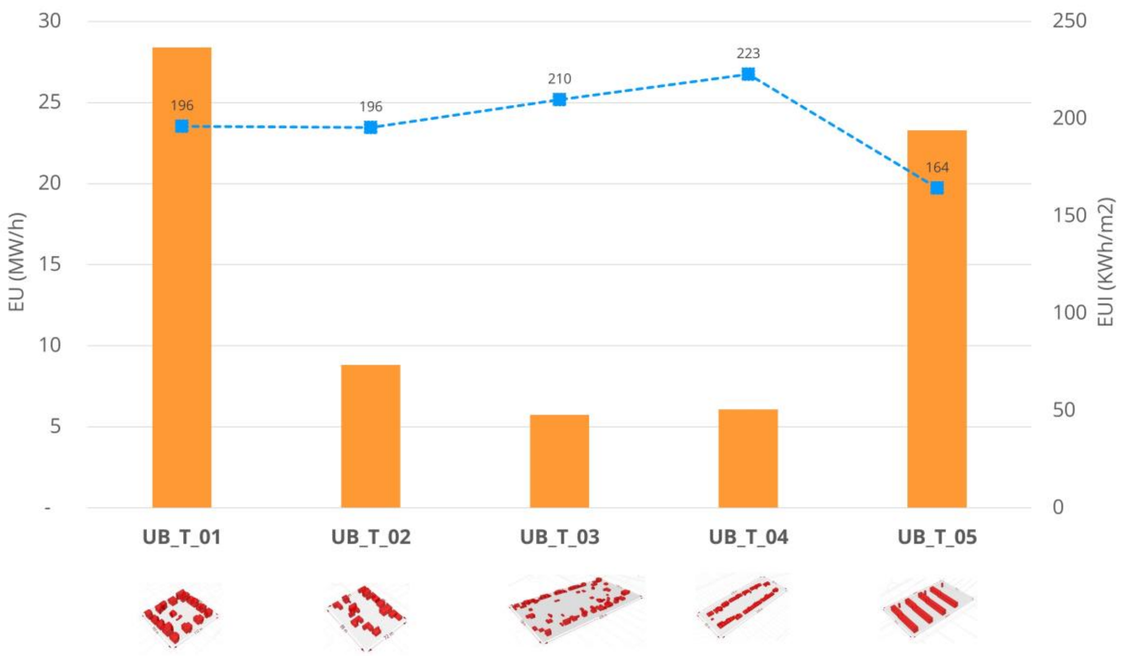

Figure 22 Monthly EUI by energy category for each development scenario

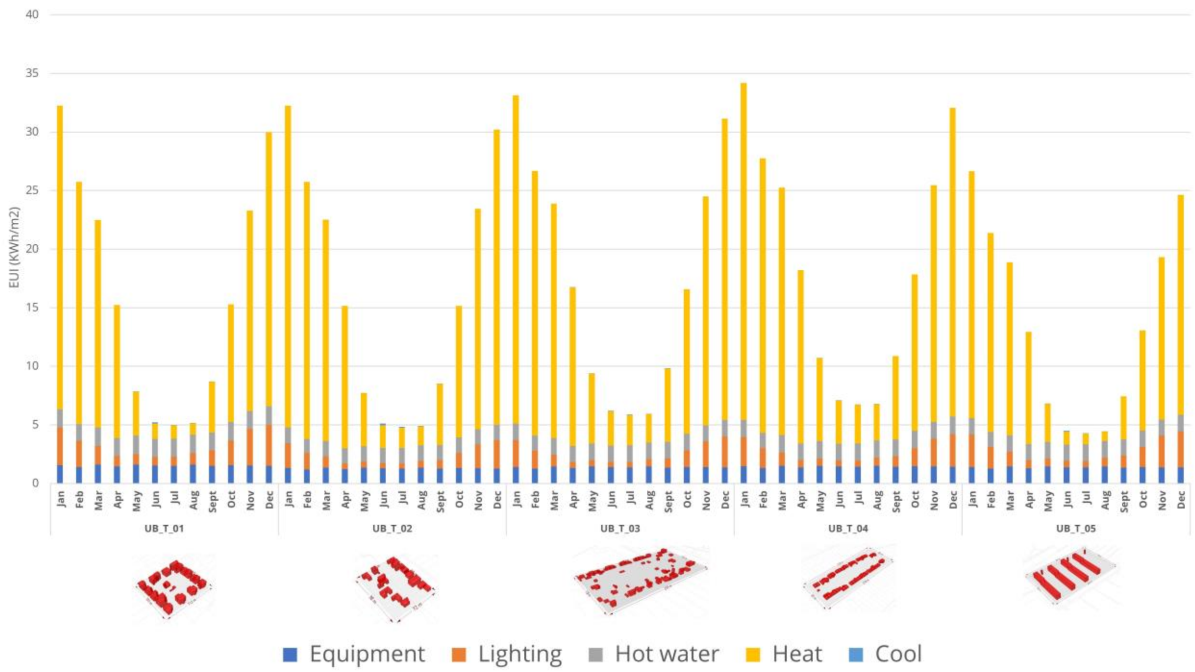

Figure 23 Relations between energy use and urban parameters

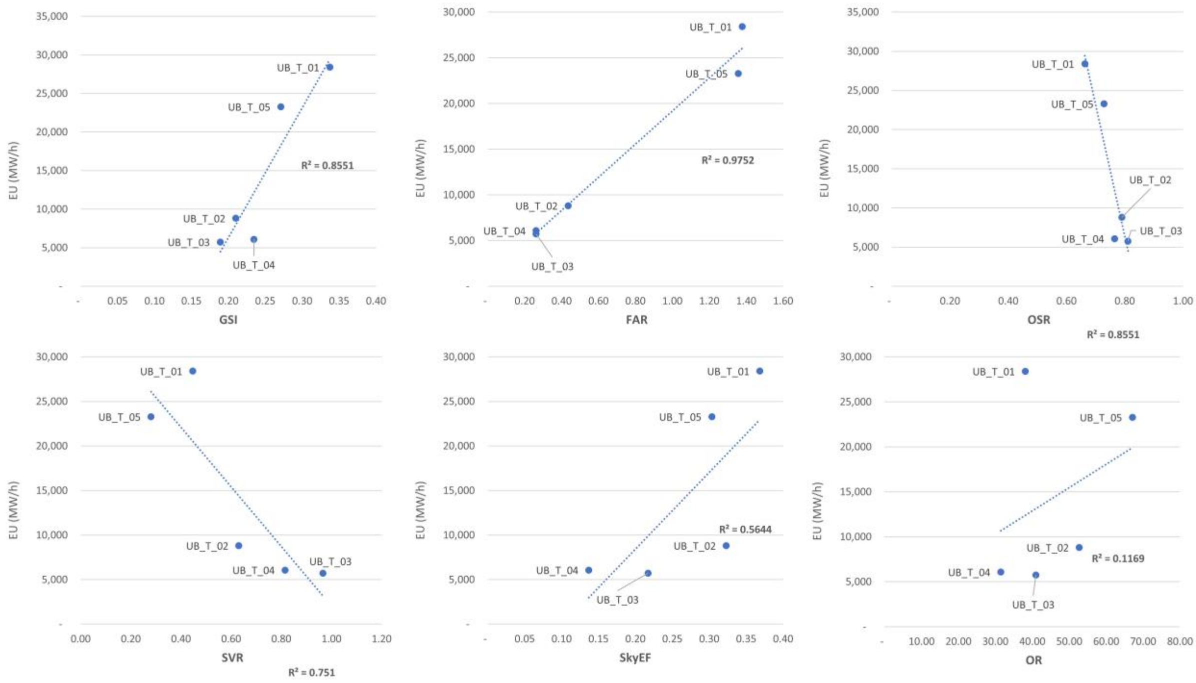

Figure 24 Influence of urban and geometric parameters on performance indicators

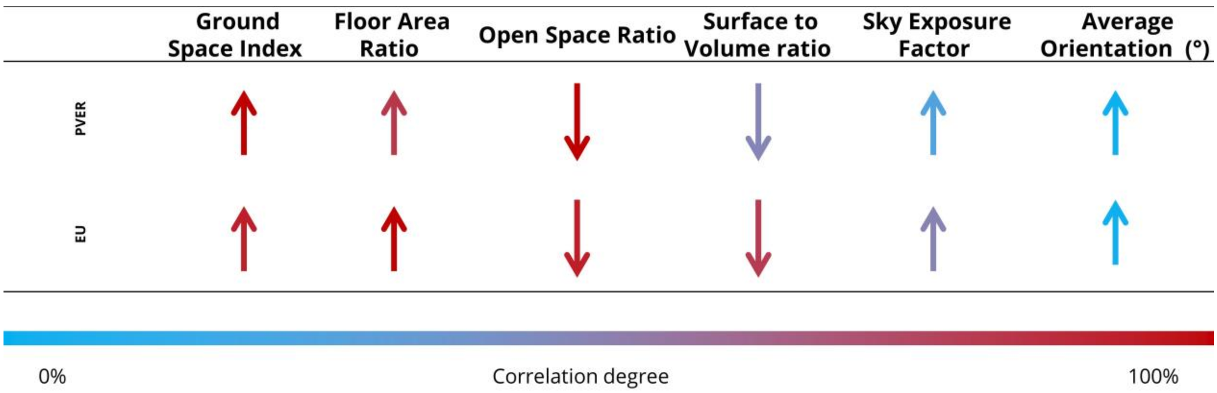

3.3 Urban development assessment

In this section, the urban development assessment will be described, considering the PVE and EUI. In order to compare the results between variables, a z-score distribution was used to standardize the values of both datasets (Table 2). For this calculation, the following formula was applied.

$$z - score = \frac{x - \mu}{n - 1}$$

Where x is the variable value, μ is the mean variable dataset, and n is the size of the dataset.

The EUI and the PVE normalized by GFA for each development scenario are presented in Figure 25. The comparison shows that urban typologies with high GFA (UBT01 and UBT05) have the best performance in terms of EUI but the lowest in PVE. The difference in the EUI is relatively small, with a variation of 59 kWh/ m^2 between the lowest (UBT05) and the highest (UBT04).

On the other hand, low-density typologies as UBT03 and UBT04 have the highest PVE generation per m^2, but simultaneously they display the highest energy use. Contrary to EUI, the PVE variation is four times between the highest -UBT04 with 33 kWh/ m^2- and the lowest -UBT05 with 8 kWh/ m^2.

Figure 26 shows the score assessment of each development scenario integrating EUI and PVE. In general, it can be seen that UBT05 (0.55) outperformed the other alternatives, following by the UBT04 (0.52) and UBT03 (0.52). Despite the previous, the assessment shows that the contribution and share of PVE of UBT05 and UBT01 are low compared to the other alternatives.

Figure 25 EUI and PV energy generation

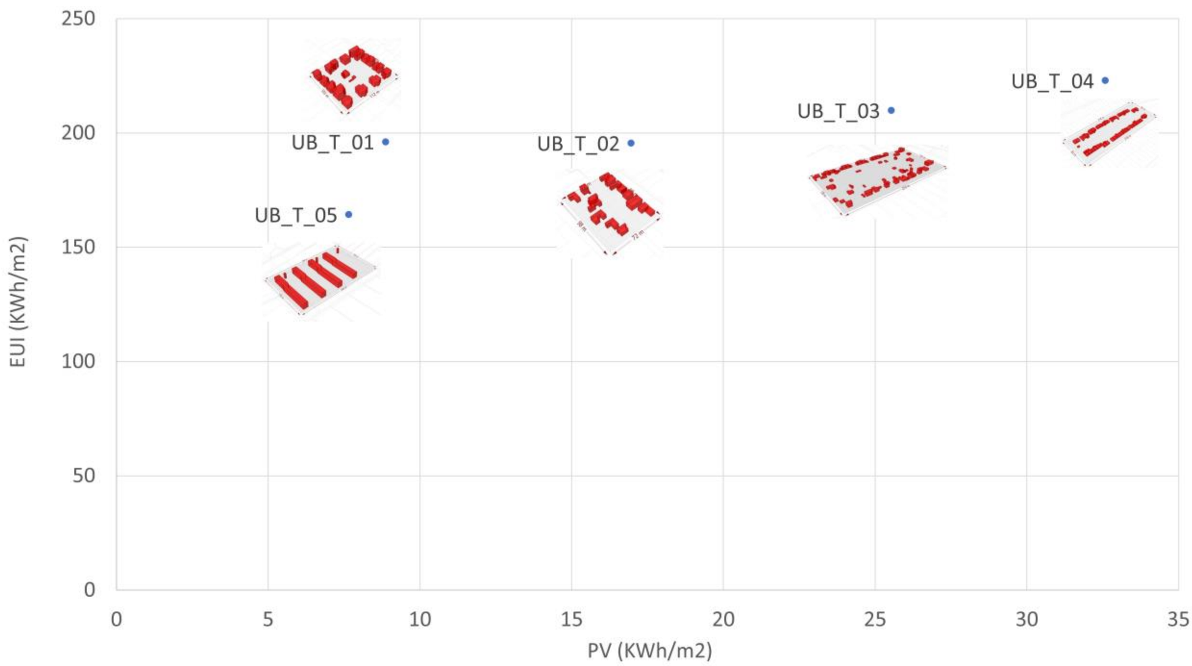

Figure 26 Assessment of each urban development scenario

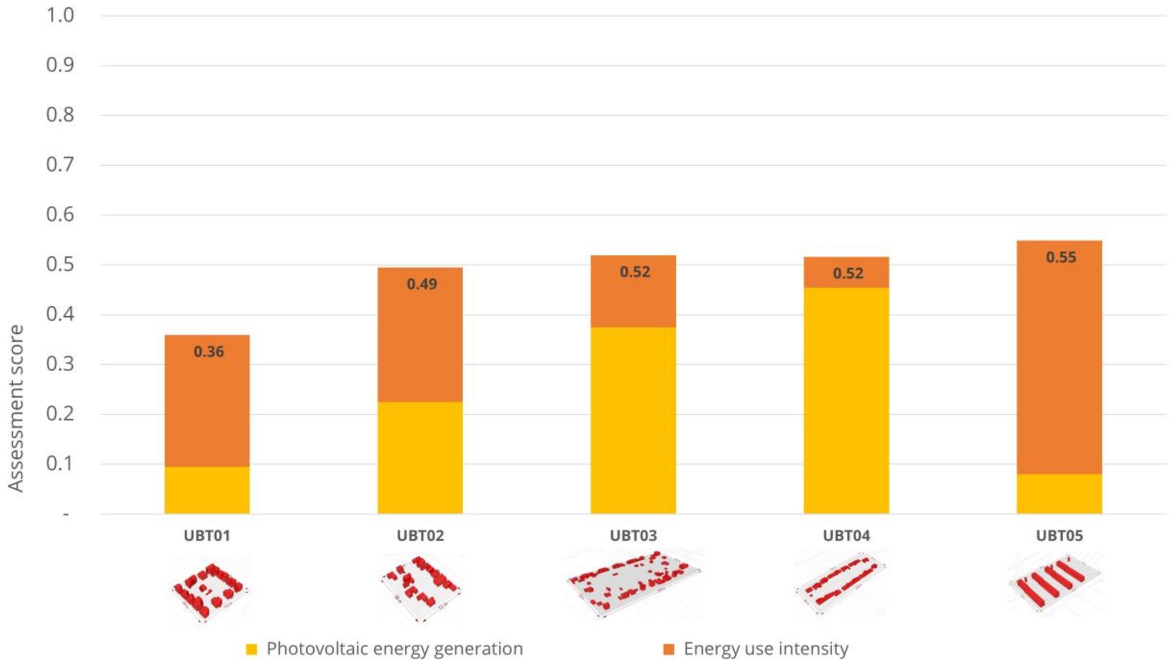

Table 2 Z-score and normal distribution calculation for each scenario

	Gross floor area (m)	Photovoltaic energy generation (kWh/m2)	Energy use intensity (kWh/m2)
UBT01	144,750.73	8.86	196.19
UBT02	45,066.35	16.96	195.59
UBT03	27,326.34	25.53	209.90
UBT04	27,257.62	32.58	222.95
UBT05	141,679.07	7.65	164.33
Mean	77,216.0	18.3	197.8
Standard deviation	60,693.6	10.7	21.8
		Z-scores	
	Gross floor area	**Photovoltaic energy generation**	**Energy use intensity**
UBT01	1.11	-0.88	-0.07
UBT02	-0.53	-0.13	-0.10
UBT03	-0.82	0.67	0.55
UBT04	-0.82	1.33	1.15
UBT05	1.06	-0.99	-1.53
		N- Distribution	
	Gross floor area	**Photovoltaic energy generation**	**Energy use intensity***
UBT01	0.87	0.19	0.53
UBT02	0.30	0.45	0.54
UBT03	0.21	0.75	0.29
UBT04	0.21	0.91	0.12
UBT05	0.86	0.16	0.94

* higher values in the normal distribution were considered as low scores

3.4 Optimization

In the previous section, five alternative urban development scenarios were assessed in terms of PVE and EUI. An ideal development scenario should provide a high energy generation (PVE) and low energy intensity (EUI). In this sense, the UBT05 outperformed the other alternatives; however, along with UBT01, they recorded one of the lowest PVE shares. The UBT05 generated 1,084 MWh using 87% of its suitable surface for solar harvesting. On the other hand, UBT01 showed the greatest need for improvement in solar harvesting potential since only 70% of its building envelope was considered roof surface and effectively used for PV deployment.

At this point, the energy performance optimization can target the reduction of the building energy use for UBT04 or the increase of renewable energy generation for UBT01. The reduction of energy use intensity implies having a larger gross floor area either by increasing the building footprint or the number of buildings storeys. Considering the relations in Figure 23, increasing the GFA will simultaneously raise the building energy use; therefore, the optimization of UBT04 will likely reduce the share of renewable energy in the urban development scenario.

The optimization of PVE involves incrementing either the footprint area or suitable surface for PV deployment. Around 30% of the appropriate surface for solar harvesting in UBT01 was not considered for the PVE simulations. By enabling facades and vertical walls for PV deployment, the energy generation might increase without a significant burden on the current energy use, which eventually might improve the share of renewable energy sources.

Taking into account the previous, in this section, the optimization of solar harvesting potential for the UBT01 was carried out considering facades and walls of the building envelope. Different building orientations were analyzed since the mutual shading effect of external buildings might reduce the solar harvesting potential of such surfaces. The objective of this optimization was to maximize the PVE using the same solar radiation threshold and PV efficiency as stated in section 2.3.2. Though facades and wall surfaces will be analyzed to know the amount of solar radiation, a window-to-wall ratio of 0.30 was set, allowing 70% of façade and wall surfaces to effectively being used for PV deployment (Figure 27). The building geometries of UBT01 were rotated on the centroid-axis as a group. The rotation angle was kept between -90 and 90 degrees to reduce the simulation time. A rotation interval was set every 10 degrees to record significant differences in solar harvesting potential. Thus, 18 different rotated alternatives of UBT01 were analyzed for solar radiation and PV energy generation.

Figure 27 Optimized model at -20° considering roof and façade surfaces

Table 3 Parameters for the base and optimized alternative of UBT01

	Ground Space Index	Floor Area Ratio	Open Space Ratio	Orientation	Ground Floor Area (m)	Sky Exposure Factor (%)	Surface to Volume Ratio	PVER (kWh)	PVER normalized by GFA (KWh/m2)	PV Surface (m)	PV Roof (m)	PV normalized by roof area (KWh/m2)
UB_T_01	0.34	1.38	0.66	38.07	144,751	0.37	0.45	1,282,882	9	48,467	35,452	36
UBT01_Opt	0.33	1.41	0.67	32.75	147,969	0.50	0.36	9,278,747	63	45,290	34,661	268

Figure 28 illustrates the general increase in energy generation assuming the deployment of PV on all suitable surfaces. Table 3 shows the comparison between the base and optimized scenario and supports the following observations. First, considering the façades for energy generation in the base scenario (0° rotation), the PVE registered 6,4 times more energy (8,227 MWh). Second, the urban development scenario with the highest PV generation was found at a -20° rotation angle, which reported 9,279 MWh representing 7,2 times the base scenario. Here is noteworthy that despite taking into account façade and roof surfaces, it is estimated that only 80% of the suitable cover for solar harvesting is producing energy due to the fenestration constraint.

Regarding the urban and geometric indicators, most of the parameters remain similar to the base scenario; there are slight differences due to the rotation of the objects could imply an increase or reduction of building footprints.

In Figure 29, the overall scores were adjusted, integrating the optimized scenario results with the other alternatives. The new assessment indicates that the optimized scenario outperforms the original options and suggests the critical role of the façade for PV energy generation.

Table 3 Parameters for the base and optimized alternative of UBT01

	Ground Space Index	Floor Area Ratio	Open Space Ratio	Orientation	Ground Floor Area (m)	Sky Exposure Factor (%)	Surface to Volume Ratio	PVER (kWh)	PVER normalized by GFA (KWh/m2)	PV Surface (m)	PV Roof (m)	PV normalized by roof area (KWh/m2)
UB_T_01	0.34	1.38	0.66	38.07	144,751	0.37	0.45	1,282,882	9	48,467	35,452	36
UBT01_Opt	0.33	1.41	0.67	32.75	147,969	0.50	0.36	9,278,747	63	45,290	34,661	268

Figure 28 PV results for each optimization scenario

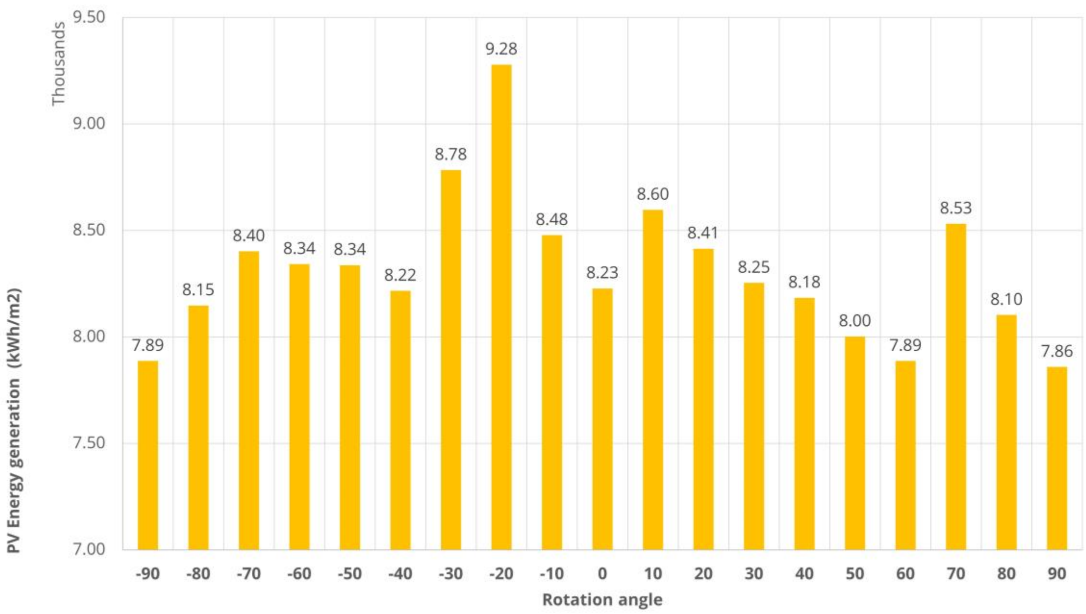

Figure 29 Assessment of urban development scenarios, including optimization scenario.

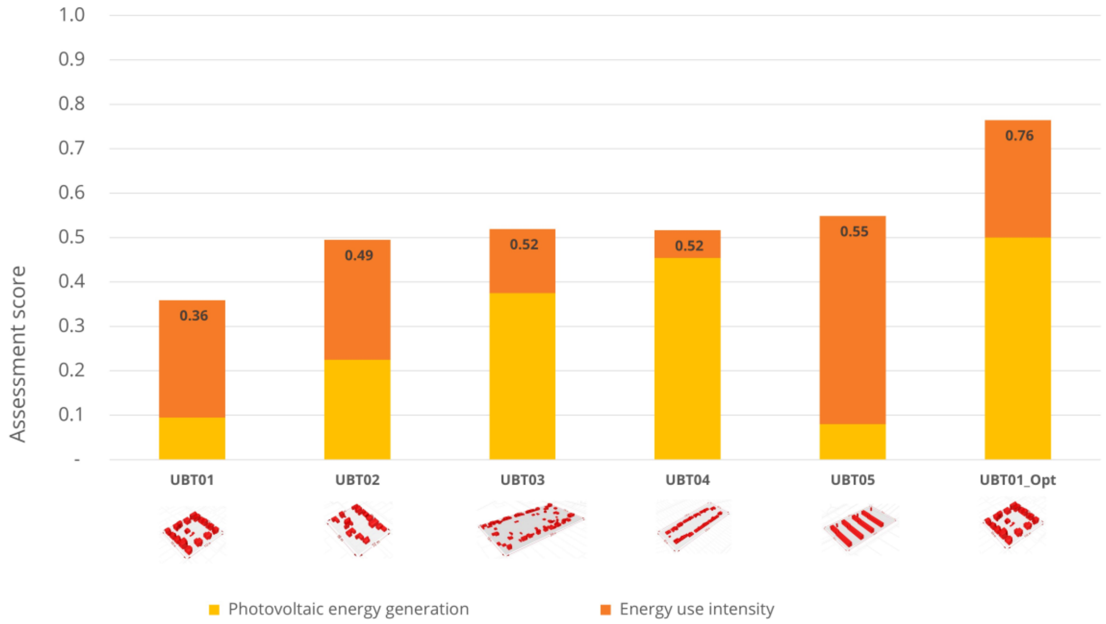

4 Discussion

4.1 Urban development and energy use

The results of the energy simulations for the five proposed urban development scenarios present significant variations in the total energy use. More specifically, those scenarios with the biggest GFA register up to 5 times more energy than those with a smaller GFA. Following the previous, the urban parameters with more relevancy to the building energy use are the GSI and FAR as they involve the floor area increase. However, the energy use intensity reveals the more significant impact of scattered development scenarios based on UBT03 and UBT04 in terms of energy use. Despite the previous, disperse urban development scenarios have less total energy consumption and a more significant share of renewable power as an energy source than other scenarios (Table 4).

4.2 Urban development and solar harvesting potential

Even though the solar harvesting potential exhibits differences in terms of the total energy generated by PV, particularly between UBT03 and UBT01, significant variations are observed for the PVE normalized by the gross floor area (Figure 18). Here the UBT04 outperforms the other alternatives. Since the roof area was considered as the surface that effectively produced energy, the GSI was found the most relevant urban parameter for energy generation.

Although other studies have found orientation as a critical urban parameter in the solar harvesting potential (Nault et al., 2015; Salih, 2020; Shi et al., 2021), the impact of the orientation in the first part of this analysis was not relevant. However, the surprisingly low influence of the orientation in the energy generation could be attributed to the fact that the energy generation took into account only roof areas. Since there was no significant obstruction or self-shadow effect, the orientation had little influence on the building footprint or rooftop areas and, therefore, little influence on the energy generation. Due to the optimization part, it can be identified the great influence of orientation in the PVE. The changes and variations in the buildings' rotation exhibited an influence of around 18% in the energy generation (Figure 28).

After presenting the above, the optimized urban development scenario based on a compact block typology, as the UBT01, offers the best alternative for the development of Merketal.

Table 4 Share of renewable energy

Scenario	EUI (kWh/m2)	PV normalized by GFA (kWh/m2)	PV energy share
UBT01	196.2	8.9	4.5%
UBT02	195.6	17.0	8.7%
UBT03	209.9	25.5	12.2%
UBT04	222.9	32.6	14.6%
UBT05	164.3	7.6	4.7%
UBT01_Opt	191.92	62.7	32.7%

4.3 Other considerations

Dispersed urban block typologies as UBT03 and UBT04 might offer less sealed surface and have relative energy generation advantages but less space for housing, making urbanization and construction costs more expensive than compact scenarios. In addition to the previous, since the project site is located relatively outside the city, a low-density development could bring a higher impact in terms of mobility -e.g., transportation mode, distance traveled, speed traveled- (Lausselet et al., 2019; Silva et al., 2017). Such urbanization costs and mobility impacts might be the subject of further research.

Regarding the objective of reaching an energy-efficient standard KfW-Effizienzhaus 40, Table 4 shows that the optimized scenario could meet a renewable energy share of 33%. Although this does not mean reducing to 60% of the building's energy use, it does mean that 33% of the energy demanded can be offset from the primary city grid and eventually reduce the city's energy demand.

4.4 Limitations

There are several limitations and observations to recognize in this work. Although the proposed urban development scenarios for Merketal might give some idea regarding energy-efficient urban development alternatives for this project, the scenarios mentioned above shouldn't be considered proper proposals of urban design since this was not the objective of this work.

Regarding the estimation of the energy use, this worked was limited to assessed and analyzed the building energy use of residential uses only. It is acknowledged that residential use is the less intense energy activity and variations in land use patterns represent differences in the energy demand (Hsieh et al., 2017). A more realistic assessment should integrate other uses and activities into the energy model. Moreover, this study was carried out only for the operational stage of the urban development without considering different phases as the LCA approach suggests. For the assessment of an energy-neutral urban development is critical to account for the energy impact of embodied and end-of-life stages and the effect of the location.(Lausselet et al., 2019; Lotteau et al., 2015)

Another limitation associated directly with the energy model is concerning the validation of the results. Although the simulation engines are recognized tools in the research field (Natanian et al., 2019), there was no actual energy consumption data of Weimar to compare the results or calibrate the energy model. Additionally, simulation inputs and parameters were kept constant for all the urban development scenarios considering standard settings (Figure 14b). Implementing passive house standards or local building templates might deliver different results. In principle, the trends might be similar because each scenario simulation used the same specific conditions, but the results' magnitude could differ from those presented here.

On the other side, the solar harvesting potential analysis was conducted assuming that roof surfaces were flat and they resembled their building footprint. Thus, this work did not consider the effect of the pitch angle on the roof surface size and the amount of solar radiation (Hailu & Fung, 2019).

Regarding the optimization, since a standard rotation angle was used to spin all the buildings uniformly, optimal solutions for individual buildings are potentially excluded. The previous means that while some buildings displayed their maximum potential at a certain rotation angle (i.e., minus 20°), it is also very likely that some others did not. Conducting individual optimization for each building or urban block could deliver more accurate PVE results and different urban development organization.

This work considered and estimated the generation of renewable energy through the deployment of PV systems; however, no financial costs were calculated to explore the feasibility of the implementation of such technology. Future works could also examine the potential for including other energy sources such as geothermal or small-scale wind turbines (Tummala et al., 2016).

5 Conclusions

This work presented the impact on solar energy harvesting potential and building energy use of alternative urban development scenarios for Merketal. The assessment was based on computational analysis of the energy use and solar radiation simulations. Five alternative scenarios representing different urban developments for the Merketal area were evaluated regarding its photovoltaic harvesting potential (PV) and energy use intensity (EUI).

The results show that under the same layout and boundary conditions, there are significant variations in EUI and PVE. Particularly, it was observed that disperse urban development composed of detached houses consumes 36% more energy than a compact multifamily buildings development scenario.

Regarding PVE, an scenario based on UBT04 presents the highest share of renewable energy source per square meter since it offers the lowest gross floor area. Regarding the suitable surface for solar harvesting, the UBT01 displays the most significant potential, delivering 46% more appropriate space for PV deployment.

The optimization of the urban scenario based on UBT01 shows the importance of the orientation in passive strategies and reveals the potential contribution of facades and walls for solar harvesting. The UBT01 exhibits the most significant potential for the deployment of PV systems on building's facades since 23% of its suitable surface for solar harvesting is consider wall surface. Enabling the facades for energy generation in such a scenario produces around six times more energy than only using roof areas. On top of that, optimizing the building's orientation reveals that the total energy generation improves by 13% with a rotation angle of -20°.

Finally, the explored correlations between the planning and geometric parameters of such scenarios and their energy performance disclosed the significant influence of GSI and FAR both on energy use and solar harvesting potential. However, it is seen that the GSI has a more significant effect on the PVE while the FAR on the energy use.

6 References

1. Adalberth, K. (1997). Energy use during the life cycle of single-unit dwellings: Examples. *Building and Environment*, *32*(4), 321–329. https://doi.org/10.1016/S0360-1323(96)00069-8

2. Altan, H., Hajibandeh, M., Tabet Aoul, K. A., & Deep, A. (2016). Passive Design. In M. Noguchi (Ed.), *ZEMCH: Toward the Delivery of Zero Energy Mass Custom Homes* (pp. 209–236). Springer International Publishing. https://doi.org/10.1007/978-3-319-31967-4_8

3. Anderson, J. E., Wulfhorst, G., & Lang, W. (2015). Energy analysis of the built environment—A review and outlook. *Renewable and Sustainable Energy Reviews*, *44*, 149–158. https://doi.org/10.1016/j.rser.2014.12.027

4. Araji, M. T. (2019). Surface-to-volume ratio: How building geometry impacts solar energy production and heat gain through envelopes. *IOP Conference Series: Earth and Environmental Science*, *323*, 012034. https://doi.org/10.1088/1755-1315/323/1/012034

5. Asarpota, K., & Nadin, V. (2020). Energy Strategies, the Urban Dimension, and Spatial Planning. *Energies*, *13*(14), 3642. https://doi.org/10.3390/en13143642

6. Berghauser Pont, M. Y., & Haupt, P. A. (2009). *Space, density and urban form.* s.n.

7. Bröde, P., Krüger, E., & Rossi, F. (2011). *ASSESSMENT OF URBAN OUTDOOR THERMAL COMFORT BY THE UNIVERSAL THERMAL CLIMATE INDEX UTCI*.

8. Climate.OneBuilding.Org. (2021). *EPW Weimar*. http://climate.onebuilding.org/WMO_Region_6_Europe/DEU_Germany/index.html

9. Dec, E., Babiarz, B., & Sekret, R. (2018). Analysis of temperature, air humidity and wind conditions for the needs of outdoor thermal comfort. *E3S Web of Conferences*, *44*, 00028. https://doi.org/10.1051/e3sconf/20184400028

10. Dempsey, N., Brown, C., Raman, S., Porta, S., Jenks, M., Jones, C., & Bramley, G. (2008). Elements of Urban Form. In M. Jenks & C. Jones (Eds.), *Sustainable City Form* (Vol. 2, pp. 21–51). Springer Netherlands. https://doi.org/10.1007/978-1-4020-8647-2_2

11. Ghazi, S., & Ip, K. (2014). The effect of weather conditions on the efficiency of PV panels in the southeast of UK. *Renewable Energy*, *69*, 50–59. https://doi.org/10.1016/j.renene.2014.03.018

12. Hailu & Fung. (2019). Optimum Tilt Angle and Orientation of Photovoltaic Thermal System for Application in Greater Toronto Area, Canada. *Sustainability*, *11*(22), 6443. https://doi.org/10.3390/su11226443

13. Hemsath, T. L. (2016). Housing orientation's effect on energy use in suburban developments. *Energy and Buildings*, *122*, 98–106. https://doi.org/10.1016/j.enbuild.2016.04.018

14. Hsieh, S., Schüler, N., Shi, Z., Fonseca, J. A., Marechal, F., & Schlueter, A. (2017). *Defining density and land uses under energy performance targets at the early stage of urban planning processes* [Application/pdf]. https://doi.org/10.3929/ETHZ-B-000185715

15. Kang, J., Ahn, K., Park, C., & Schuetze, T. (2015). Assessment of Passive vs. Active Strategies for a School Building Design. *Sustainability*, *7*(11), 15136–15151. https://doi.org/10.3390/su71115136

16. Kottek, M., Grieser, J., Beck, C., Rudolf, B., & Rubel, F. (2006). World Map of the Köppen-Geiger climate classification updated. *Meteorologische Zeitschrift*, *15*(3), 259–263. https://doi.org/10.1127/0941-2948/2006/0130

17. Lausselet, C., Borgnes, V., & Brattebø, H. (2019). LCA modelling for Zero Emission Neighbourhoods in early stage planning. *Building and Environment*, *149*, 379–389. https://doi.org/10.1016/j.buildenv.2018.12.034

18. Littlefair, P. (1998). Passive solar urban design: Ensuring the penetration of solar energy into the city. *Renewable and Sustainable Energy Reviews*, *2*(3), 303–326. https://doi.org/10.1016/S1364-0321(97)00009-9

19. Loga, T., Stein, B., Diefenbach, N., Born, R., & Institut Wohnen und Umwelt (Eds.). (2015). *Deutsche Wohngebäudetypologie: Beispielhafte Maßnahmen zur Verbesserung der Energieeffizienz von typischen Wohngebäuden ; erarbeitet im Rahmen der EU-Projekte TABULA - "Typology approach for building stock energy assessment", EPISCOPE - "Energy performance indicator tracking schemes for the continous optimisation of refurbishment processes in European housing stocks"* (2., erw. Aufl). IWU.

20. Lotteau, M., Yepez-Salmon, G., & Salmon, N. (2015). Environmental Assessment of Sustainable Neighborhood Projects through NEST, a Decision Support Tool for Early Stage Urban Planning. *Procedia Engineering*, *115*, 69–76. https://doi.org/10.1016/j.proeng.2015.07.356

21. Lylykangas, K. (2009). *Shape Factor as an Indicator of Heating Energy Demand*. 8.

22. Müller, D. (2020). *Energiewendebauen. Forschungserkenntnisse von der Komponente bis zum Quartier.* Fraunhofer IRB-Verlag.

23. Natanian, J. (2018). *Zero Energy Buildings in the Mediterranean: Typological Feasibility Analysis towards an Israeli Adaptation*.

24. Natanian, J., Aleksandrowicz, O., & Auer, T. (2019). A parametric approach to optimizing urban form, energy balance and environmental quality: The case of Mediterranean districts. *Applied Energy*, *254*, 113637. https://doi.org/10.1016/j.apenergy.2019.113637

25. Natanian, J., & Wortmann, T. (2021). Simplified evaluation metrics for generative energy-driven urban design: A morphological study of residential blocks in Tel Aviv. *Energy and Buildings*, *240*, 110916. https://doi.org/10.1016/j.enbuild.2021.110916

26. Nault, E., Peronato, G., Rey, E., & Andersen, M. (2015). Review and critical analysis of early-design phase evaluation metrics for the solar potential of neighborhood designs. *Building and Environment*, *92*, 679–691. https://doi.org/10.1016/j.buildenv.2015.05.012

27. Oliveria, V., & Silva, M. (2013). *Urban form and energy*. Urban Morphol. 17. http://www.urbanform.org/online_unlimited/pdf2013/201317_45.pdf

28. Quan, S. J., & Li, C. (2021). Urban form and building energy use: A systematic review of measures, mechanisms, and methodologies. *Renewable and Sustainable Energy Reviews*, *139*, 110662. https://doi.org/10.1016/j.rser.2020.110662

29. Salih, K. (2020). Impact of the Design of Urban Block on Buildings' Indoor Daylight and Energy Loads in Semi-Arid Regions. In H. Bougdah, A. Versaci, A. Sotoca, F. Trapani, M. Migliore, & N. Clark (Eds.), *Urban and Transit Planning* (pp. 575–589). Springer International Publishing. https://doi.org/10.1007/978-3-030-17308-1_50

30. Shi, Z., Fonseca, J. A., & Schlueter, A. (2017). A review of simulation-based urban form generation and optimization for energy-driven urban design. *Building and Environment*, *121*, 119–129. https://doi.org/10.1016/j.buildenv.2017.05.006

31. Shi, Z., Fonseca, J. A., & Schlueter, A. (2021). A parametric method using vernacular urban block typologies for investigating interactions between solar energy use and urban design. *Renewable Energy*, *165*, 823–841. https://doi.org/10.1016/j.renene.2020.10.067

32. Silva, M., Oliveira, V., & Leal, V. (2017). Urban Form and Energy Demand: A Review of Energy-relevant Urban Attributes. *Journal of Planning Literature*, *32*(4), 346–365. https://doi.org/10.1177/0885412217706900

33. Solemma LLC. (2021). *Welcome to the ClimateStudio User Guide—ClimateStudio latest documentation* [User Guide]. Welcome to the ClimateStudio User Guide. https://climatestudiodocs.com/index.html

34. Soukka, R., Väisänen, S., Grönman, K., Uusitalo, V., & Kasurinen, H. (2020). Life Cycle Assessment. In S. Idowu, R. Schmidpeter, N. Capaldi, L. Zu, M. Del Baldo, & R. Abreu (Eds.), *Encyclopedia of Sustainable Management* (pp. 1–10). Springer International Publishing. https://doi.org/10.1007/978-3-030-02006-4_623-1

35. Stadt Weimar. (2011). *Integriertes Klimaschutzkonzept Strom, Wärme, Kälte der Stadt Weimar*. Stadt Weimar.

36. Stadt Weimar. (2020). *Änderungsantrag zur DS 2020/302/V - Städtebaulicher Grundvertrag zur Entwicklung des Wohnbaugebietes „Im Merketale II"*.

37. Stein, J. S., Hansen, C. W., & Reno, M. J. (2012). *Global horizontal irradiance clear sky models: Implementation and analysis.* (No. SAND2012-2389, 1039404; pp. SAND2012-2389, 1039404). https://doi.org/10.2172/1039404

38. Tuladhar, R., & Yin, S. (2019). Sustainability of using recycled plastic fiber in concrete. In *Use of Recycled Plastics in Eco-efficient Concrete* (pp. 441–460). Elsevier. https://doi.org/10.1016/B978-0-08-102676-2.00021-9

39. Tummala, A., Velamati, R. K., Sinha, D. K., Indraja, V., & Krishna, V. H. (2016). A review on small scale wind turbines. *Renewable and Sustainable Energy Reviews*, *56*, 1351–1371. https://doi.org/10.1016/j.rser.2015.12.027

40. Yang, C., & Choi, J.-H. (2015). Energy Use Intensity Estimation Method Based on Façade Features. *Procedia Engineering*, *118*, 842–852. https://doi.org/10.1016/j.proeng.2015.08.522

41. Zarco-Soto, I. M., Zarco-Periñán, P. J., & Sánchez-Durán, R. (2020). Influence of climate on energy consumption and CO2 emissions: The case of Spain. *Environmental Science and Pollution Research*, *27*(13), 15645–15662. https://doi.org/10.1007/s11356-020-08079-7

42. Zhang, J., Heng, C. K., Malone-Lee, L. C., Hii, D. J. C., Janssen, P., Leung, K. S., & Tan, B. K. (2012). Evaluating environmental implications of density: A comparative case study on the relationship between density, urban block typology and sky exposure. *Automation in Construction*, *22*, 90–101. https://doi.org/10.1016/j.autcon.2011.06.011

43. Zhang, J., Xu, L., Shabunko, V., Tay, S. E. R., Sun, H., Lau, S. S. Y., & Reindl, T. (2019). Impact of urban block typology on building solar potential and energy use efficiency in tropical high-density city. *Applied Energy*, *240*, 513–533. https://doi.org/10.1016/j.apenergy.2019.02.033

44. Icons Figure 1 Methodology
    a. Data by Gregor Cresnar from the Noun Project
    b. Modeling by Serhii Smirnov from the Noun Projec
    c. Performance by Lima Studio from the Noun Project
    d. Optimization by Gregor Cresnar from the Noun Project
    e. Result by Adrien Coquet from the Noun Project

7 Annex

UBT01
Building energy use per year
Zone People Total Heating Energy, Zone Lights Electricity Energy, Electric Equipment Electricity Energy, Zone Electric Equipment Electricity Energy, Water Use Equipment Heating Energy.
56 kWh/m2
155 kWh/m2
Monthly building energy use per category
Total EU (MWh)
5,000
4,500
4,000
3,500
3,000
2,500
2,000
1,500
1,000
500
0
Sum of Jan
Sum of Feb
Sum of Mar
Sum of Apr
Sum of May
Sum of Jun
Sum of Jul
Sum of Aug
Sum of Sept
Sum of Oct
Sum of Nov
Sum of Dec
Equipment
Fans
Lights
Hot Water
Heat
Cool
Solar radiation per year
1 kWh/m2
1286 kWh/m2
Frequency distribution
Thousands
Amount of Surface (m2)
36.58
27.83
24.70
11.16
10.45
9.25
7.98
7.12
6.39
5.75
5.50
> 1000
< 100
101 to 200
701 to 800
601 to 700
501 to 600
201 to 300
401 to 500
801 to 900
301 to 400
901 to 1000
Solar radiation interval

UBT02

Building energy use per year

Zone People Total Heating Energy, Zone Lights Electricity Energy, Electric Equipment Electricity Energy, Zone Electric Equipment Electricity Energy, Water Use Equipment Heating Energy.

32 kWh/m2 133 kWh/m2

Monthly building energy use per category

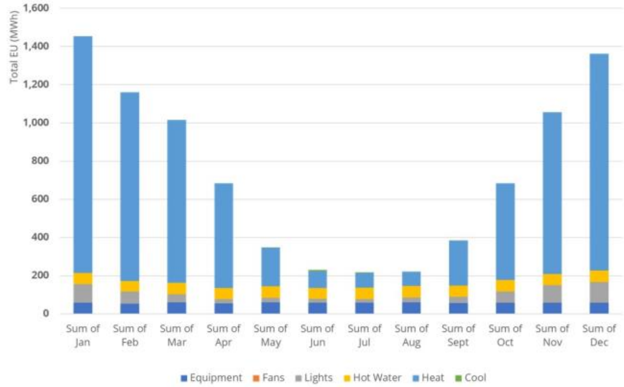

Solar radiation per year

1 kWh/m2 1289 kWh/m2

Frequency distribution

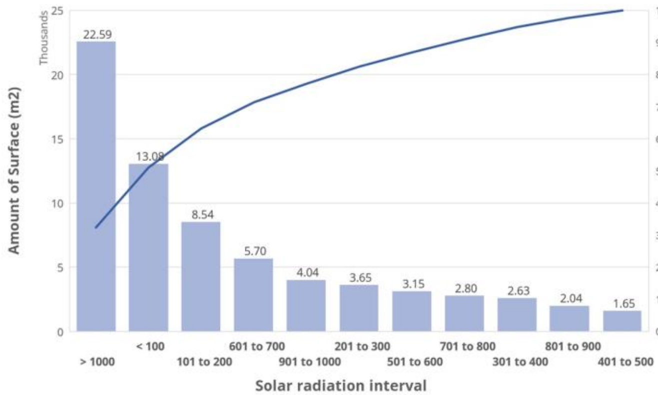

UBT03

Building energy use per year

Zone People Total Heating Energy, Zone Lights Electricity Energy, Electric Equipment Electricity Energy, Zone Electric Equipment Electricity Energy, Water Use Equipment Heating Energy.

14 kWh/m2 — 493 kWh/m2

Monthly building energy use per category

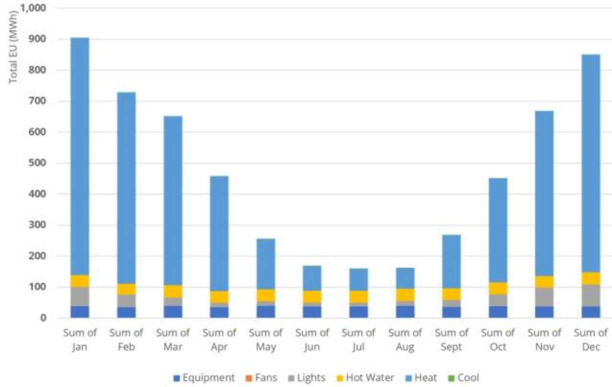

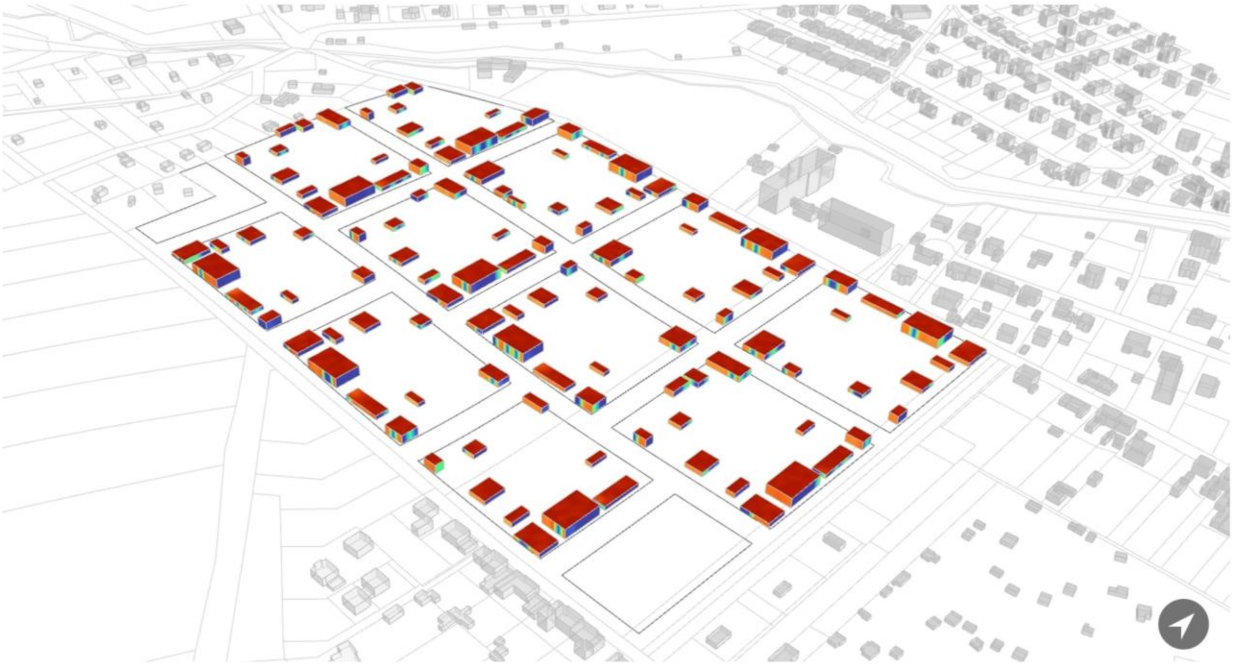

Solar radiation per year

1 kWh/m2 — 1293 kWh/m2

Frequency distribution

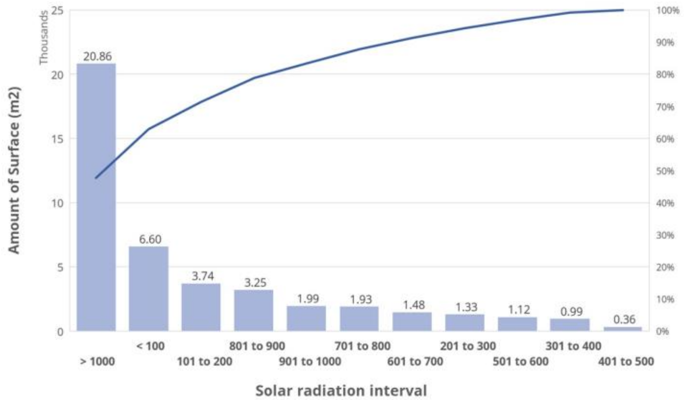

UBT04

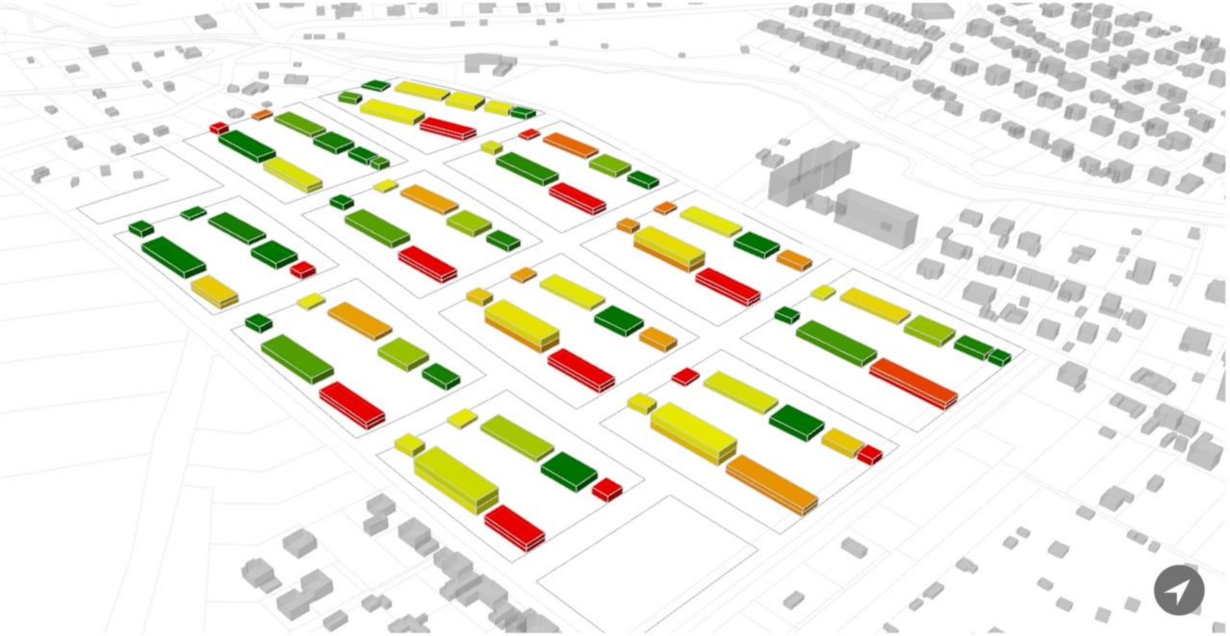

Building energy use per year

Zone People Total Heating Energy, Zone Lights Electricity Energy, Electric Equipment Electricity Energy, Zone Electric Equipment Electricity Energy, Water Use Equipment Heating Energy.

68 kWh/m2 75 kWh/m2

Monthly building energy use per category

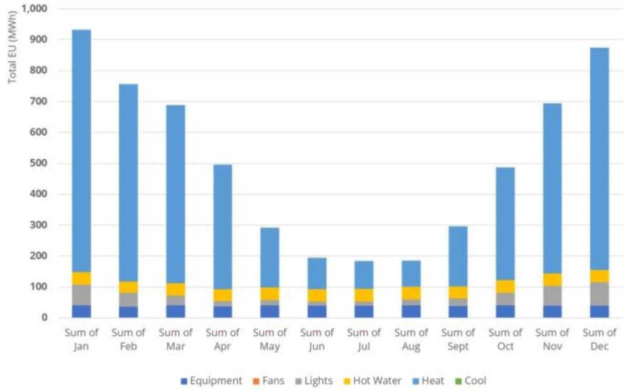

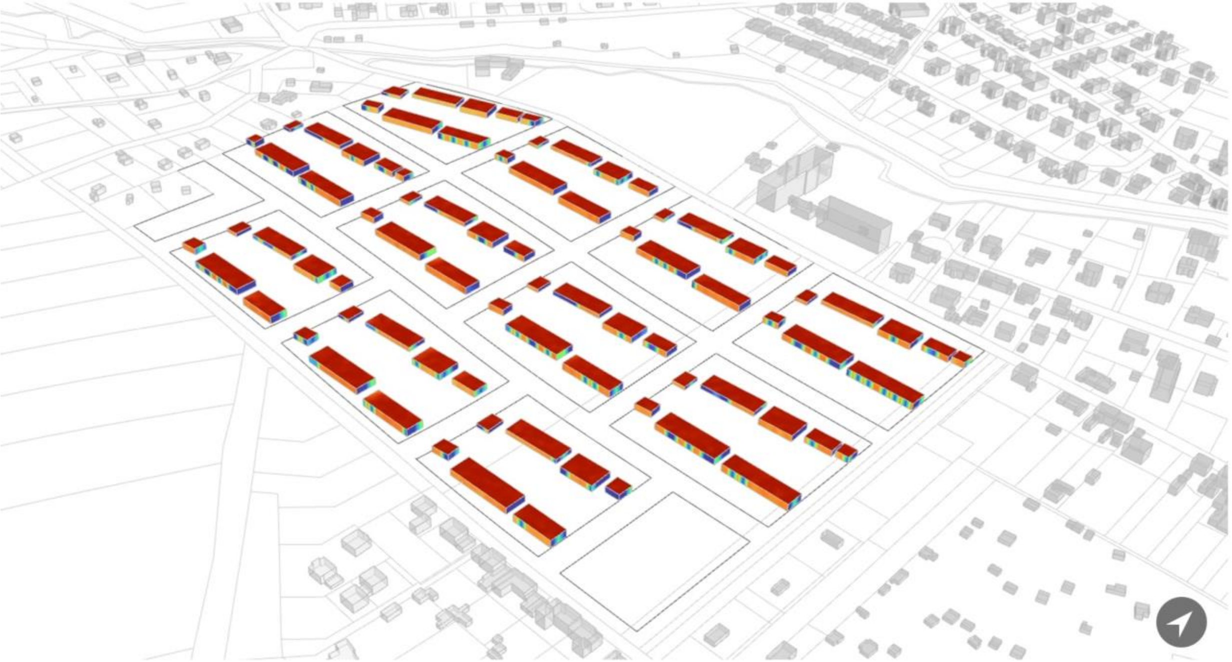

Solar radiation per year

2 kWh/m2 1289 kWh/m2

Frequency distribution

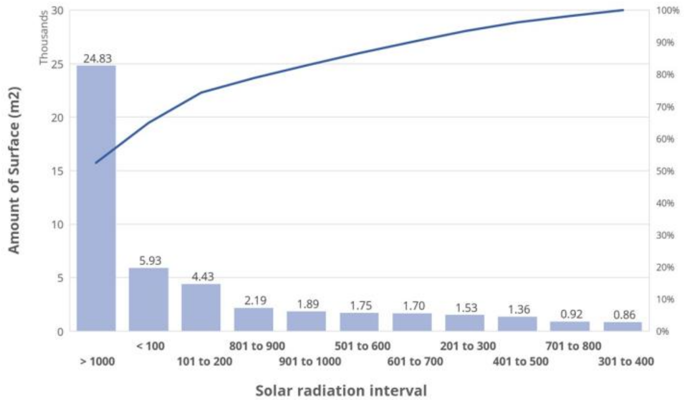

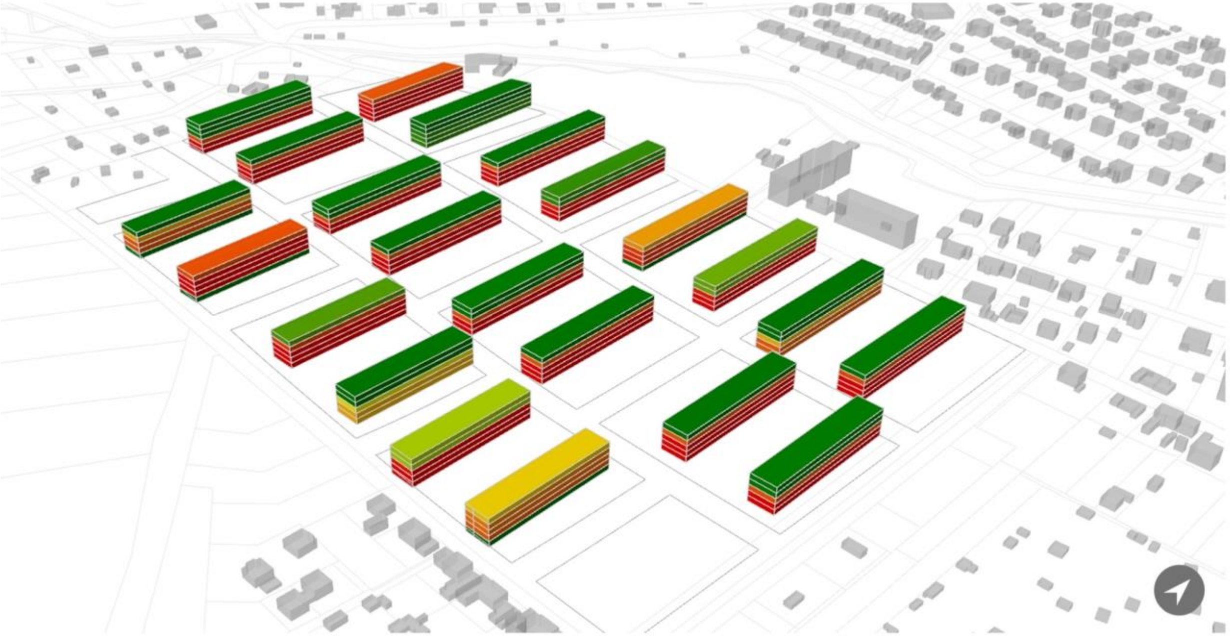

UBT05

Building energy use per year

Zone People Total Heating Energy, Zone Lights Electricity Energy, Electric Equipment Electricity Energy, Zone Electric Equipment Electricity Energy, Water Use Equipment Heating Energy.

80 kWh/m2 83 kWh/m2

Monthly building energy use per category

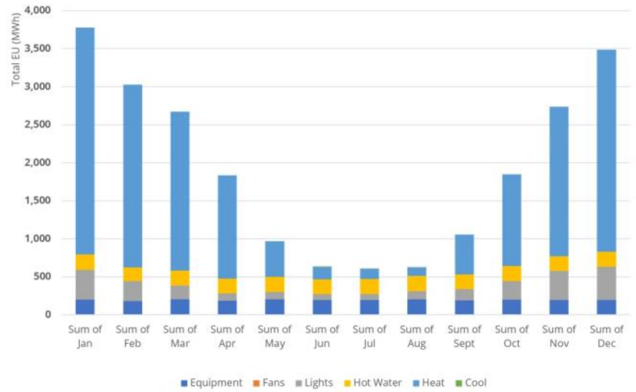

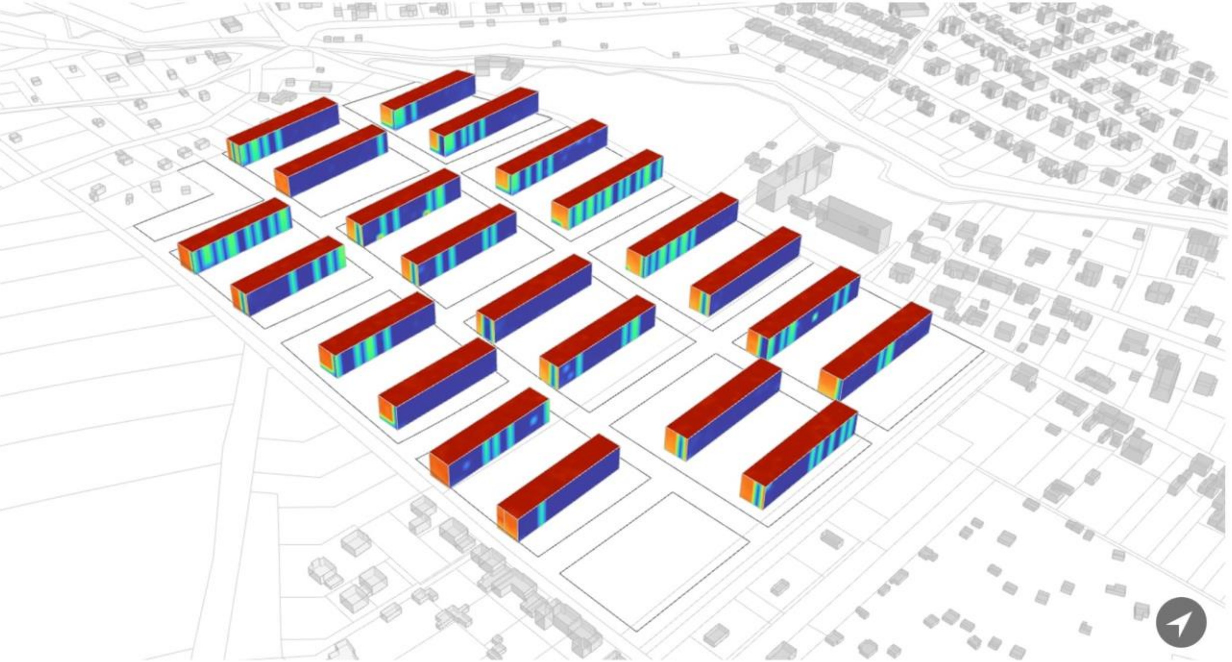

Solar radiation per year

56 kWh/m2 155 kWh/m2

Frequency distribution

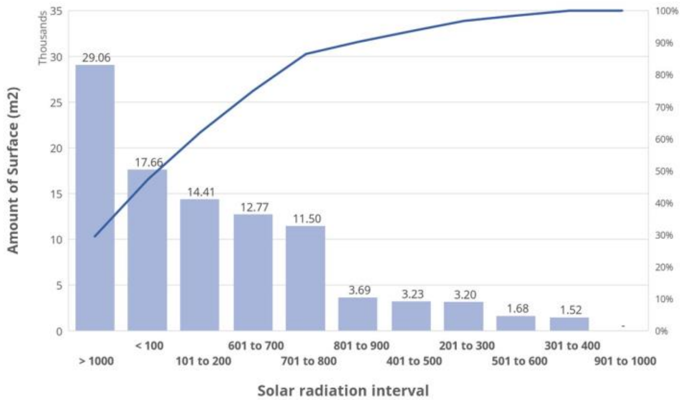

Statutory Declaration

I hereby affirm that the Master thesis at hand is my own written work and that I have used no other sources and aids other than those indicated. All passages, which are quoted from publications or paraphrased from these sources, are indicated as such, i.e., cited, attributed.

I am aware that my thesis can be entered in a database after the examination period for future comparison with other works and to contribute to knowledge dissemination. Further rights of reproduction are, however, not granted here and should be requested to the author.

This thesis was not submitted in the same or in a substantially similar version, not even partially, to another examination board and was not published elsewhere.

Also, I would like to thank my supervisors Sven Schneider and Martin Bielik for the guidance and feedback throughout this process. I'm also very grateful to my family, and beloved ones who ,from afar, were days and nights supporting me during this phase.

Auf das was kommt und das was war

Weimar, 23th August 2021

Place, Date

Signature (First name and Surname)